Elsevier required licence: © 2021

This manuscript version is made available under the CC-BY-NC-ND 4.0 license

http://creativecommons.org/licenses/by-nc-nd/4.0/

The definitive publisher version is available online at

https://doi.org/10.1016/j.trgeo.2021.100517

Transportation Geotechnics

Large-scale Testing Facility for Heavy Haul Track

--Manuscript Draft--

Manuscript Number:	TRGEO-D-20-00552R2
Article Type:	Original article
Keywords:	Ballast; Rail geotechnics; Heavy hauls; breakage; Prototype test
Corresponding Author:	Buddhima Indraratna, PhD (Alberta), FTSE, FASCE University of Technology Sydney Sydney, NSW AUSTRALIA
First Author:	Buddhima Indraratna
Order of Authors:	Buddhima Indraratna
	Trung Ngo, PhD
	Fernanda Bessa Ferreira, PhD
	Cholachat Rujikiatkamjorn, PhD
	Ameyu Tucho, PhD student
Manuscript Region of Origin:	Europe
Abstract:	Given the substantially increased demand for increased axle loads of heavy haul trains, there is an imperative need to develop sustainable track infrastructure. When subjected to heavy axle loading, ballast aggregates rapidly break down, compromising the particle friction and associated load bearing capacity. Therefore, understanding the deformation and degradation (breakage) of ballast subjected to various boundary and loading conditions is crucial for improved track design and performance monitoring. Ideally, field testing should be carried out in real-life tracks to avoid laboratory scale and boundary effects, but field tests are often expensive, time-consuming and may disrupt rail traffic, hence not always feasible. A prototype test facility that can simulate appropriate axle loading and boundary conditions for standard gauge heavy haul tracks is presented in this paper. In collaboration with more than a dozen Universities and Industry organisations, Australia's first and only National Facility for Heavy-haul Railroad Testing (NFHRT) has recently been constructed and is now fully operational. This new facility enables a real-size (1:1 scale) instrumented track section to be subjected to continuous cyclic loading simulated via two pairs of dynamic actuators in synchronized operation. The results of a typical test are presented in this paper including the measured track settlement and lateral deformation, transient vertical and lateral stresses, rail and sleeper accelerations, resilient modulus and breakage of ballast. The test results show that an average track settlement of about 14 mm and lateral displacements up to 9 mm are recorded after 500,000 load cycles. Subjected to a 25-tonne axle load, the maximum vertical stress measured at the sleeper-ballast interface is about 225 kPa and this attenuates with depth. The test results of this iconic facility are generally consistent with actual field measurements obtained in heavy-haul tracks located in the towns of Singleton and Bulli in the state of New South Wales, Australia.
Suggested Reviewers:	Arul Arulrajah, PhD Professor, Swinburne University of Technolog aarulrajah@swin.edu.au Professor Arulrajah is an expert in this area.
	Anand Puppala, PhD Professor, University of Texas (UTA) at Arlington anand@uta.edu Professor Puppala is an expert in this area.
	Eduardo Fortunato Eduardo Fortunato, PhD Professor, LNEC - Laboratório Nacional de Engenharia Civil efortunato@lnec.pt Prof Eduardo Fortunato is an expert in this area.

Powered by Editorial Manager® and ProduXion Manager® from Aries Systems Corporation

	R G Robinson, PhD Professor, Indian Institute of Technology Madras robinson@iitm.ac.in Professor Robinson is an expert in this area.
Opposed Reviewers:	
Response to Reviewers:	

Powered by Editorial Manager® and ProduXion Manager® from Aries Systems Corporation

CRediT author statement

Buddhima Indraratna: Conceptualization, Investigation, Funding, Project administration, Data analysis and interpretation, Writing-Reviewing and Editing.

Trung Ngo: Writing - original draft, Testing, Data analysis and interpretation, Investigation, Validation, Writing-Reviewing and Editing,

F. Ferreira: Conceptualization, Testing, Formal analysis, Writing - review & editing.

C. Rujikiatkamjorn: Supervision, Project administration, Conceptualization, Data analysis, Writing - review & editing.

Ameyu Tucho: Data analysis and interpretation, Writing-Reviewing and Editing

Declaration of interests

☒ The authors declare that they have no known competing financial interests or personal relationships that could have appeared to influence the work reported in this paper.

☐The authors declare the following financial interests/personal relationships which may be considered as potential competing interests:

January 13th, 2021

Transportation Geotechnics

Title: Large-scale Testing Facility for Heavy Haul Track

Authors: Buddhima Indraratna, Trung Ngo, Fernanda Bessa Ferreira, Cholachat Rujikiatkamjorn, and Ameyu Tucho

Dear Editor,

Enclosed herewith is a re-revised manuscript of the above technical paper for your consideration publishing in the Transportation Geotechnics.

Yours Sincerely,

B. Indraratne.

Buddhima Indraratna, PhD
FTSE, FIEAust, FASCE, FGS, FAusIMM, FIESL, DIC, CEng, CPEng

Distinguished Professor of Civil Engineering and Director, Transport Research Centre, University of Technology Sydney (UTS), Ultimo, NSW 2007, Australia;
Director, ARC Industrial Transformation Training Centre for Advanced Technologies in Rail Track Infrastructure (ITTC-Rail), University of Wollongong, NSW 2522, Australia.
Tel: (61 2) 4221 3046; Fax: (61 2) 4221 3293
Email: buddhima.indraratna@uts.edu.au

Manuscript File Click here to view linked References

Large-scale Testing Facility for Heavy Haul Track

Buddhima Indraratna[1], Trung Ngo[2], Fernanda Bessa Ferreira[3], Cholachat Rujikiatkamjorn[4] and Ameyu Tucho[5]

[1]Distinguished Professor of Civil Engineering and Director, Transport Research Centre, University of Technology Sydney 15 Broadway, Ultimo, NSW 2007, Australia;
Founding Director, ARC Industrial Transformation Training Centre for Advanced Technologies in Rail Track Infrastructure (ITTC-Rail), University of Wollongong, NSW 2522, Australia.
Email: Buddhima.Indraratna@uts.edu.au

[2]Senior Lecturer, School of Civil and Environmental Engineering, University of Technology Sydney, 15 Broadway, Ultimo NSW 2007, Australia. Email: Trung.Ngo@uts.edu.au

[3]Postdoctoral Researcher, CONSTRUCT-Geo, Faculty of Engineering, University of Porto, 4200-465 Porto, Portugal. Email: fbf@fe.up.pt

[4]Professor, School of Civil and Environmental Engineering, University of Technology Sydney, 15 Broadway, Ultimo NSW 2007, Australia. Program Coordinator, ARC ITTC-Rail, University of Wollongong, NSW 2522, Australia. Email: Cholachat.Rujikiatkamjorn@uts.edu.au

[5]PhD student, School of Civil and Environmental Engineering, University of Technology Sydney, 15 Broadway, Ultimo NSW 2007, Australia. Email: AmeyuTemesgen.Tucho@student.uts.edu.au

Abstract: Given the substantially increased demand for increased axle loads of heavy haul trains, there is an imperative need to develop sustainable track infrastructure. When subjected to heavy axle loading, ballast aggregates rapidly break down, compromising the particle friction and associated load bearing capacity. Therefore, understanding the deformation and degradation (breakage) of ballast subjected to various boundary and loading conditions is crucial for improved track design and performance monitoring. Ideally, field testing should be carried out in real-life tracks to avoid laboratory scale and boundary effects, but field tests are often expensive, time-consuming and may disrupt rail traffic, hence not always feasible. A prototype test facility that can simulate appropriate axle loading and boundary conditions for standard gauge heavy haul tracks is presented in this paper. In collaboration with more than a dozen Universities and Industry organisations, Australia's first and only National Facility for Heavy-haul Railroad Testing (NFHRT) has recently been constructed and is now fully operational. This new facility enables a real-size (1:1 scale) instrumented track section to be subjected to continuous cyclic loading simulated via two pairs of dynamic actuators in synchronized operation. The results of a typical test are presented in this paper including the measured track settlement and lateral deformation, transient vertical and lateral stresses, rail and sleeper accelerations, resilient modulus and breakage of ballast. The test results show that an average track settlement of about 14 mm and lateral

displacements up to 9 mm are recorded after 500,000 load cycles. Subjected to a 25-tonne axle load, the maximum vertical stress measured at the sleeper-ballast interface is about 225 kPa and this attenuates with depth. The test results of this iconic facility are generally consistent with actual field measurements obtained in heavy-haul tracks located in the towns of Singleton and Bulli in the state of New South Wales, Australia.

Keywords: *Ballast, Rail geotechnics, Heavy hauls, Breakage, Prototype test*

1. Introduction

The current track infrastructure in various parts of Australia cannot sustain the increasing demand to transport freight to and from ports in regional and rural areas. This growth in demand for faster and heavier trains leads to an increase in the frequency and load intensity on track substructure. As a result, ballasted tracks settle differentially, particularly on weak subgrades with poor drainage, they become fouled due to clay pumping and ballast breakage, and the rail tracks buckle due to insufficient confining pressures from the shoulder ballast aggregates (Suiker and Borst 2003, Zhai *et al.* 2004, Indraratna *et al.* 2016, 2020a, Sayeed and Shahin 2017, Sol-Sánchez *et al*. 2020, Powrie *et al.* 2019, Guo *et al.* 2020).

Upon repeated train loading, fouling of tracks occurs along with ballast degradation. Fouling agents could decrease the shear strength of ballast and reduce the drainage capacity of ballasted track (Indraratna *et al*. 2011, Touqan *et al.* 2020). Huang *et al.* (2009) studied track problems associated with fouling issues in Wyoming, US and found that coal dust was the worst fouling agent for its impact on track substructure and roadbed. When the coal dust fouling percentage increased, the ballast shear strength steadily decreased. In particular, wet fouling was found to exacerbate this trend. Bian *et al*. (2017) investigated track problems related to the hanging of sleepers and showed that a hanging tie would lead to an increase in dynamic impact loading on the ballast and therefore further deteriorate the track substructure. Another track problem receiving increasing attention worldwide is associated with the transition zones between a ballasted track and a concrete bridge deck leading to enhanced dynamic load, differential settlement and accelerated track degradation (Hu *et al*. 2019, Mishra *et al*. 2014, Paixão *et al*. 2016).

Previous research carried out worldwide over the past decades has shown that ballast breaks down and progressively deteriorates under freight train loading. Over the years, heavy trains and faster passenger services have caused progressive deterioration of ballast which in turn results in loss of track geometry; this compromises safety and leads to more frequent maintenance (Selig and Waters 1994, Priest *et al.* 2010, Esveld 2014, Bian *et al.* 2020). In response, Australian railway companies are now emphasising on high-speed train corridors (5 routes across NSW) and heavier freight operations (Brisbane-Melbourne Inland rail) to achieve more efficient and cost effective services, particularly in the mining and agricultural sectors. One of the major challenges in delivering heavier and faster trains in Australia is not the immediate cost, but the geotechnical problems associated with poor ground conditions and soft coastal terrain (Budiono *et al.* 2004, Powrie *et al.* 2007, Sayeed and Shahin 2016, Indraratna and Ngo 2018).

The geotechnical challenges surrounding the performance of heavy hauls and high-speed trains on ballasted railway tracks are numerous, particularly when a track profile is built along the coastal areas of Australia (Indraratna *et al.* 2018a, Cai *et al.* 2020). Typical problems that arise in track substructure include: (i) ballast breakage; (ii) mud pumping in railway tracks constructed on clays and other soft soils (Indraratna *et al.* 2020b), consisting of the upward migration of subgrade clays and fine silts (slurry) under heavy traffic loading, which promotes settlement by "lubrication" and increases the risk of train derailment (Wang *et al.* 2020); (iii) ballast fouling due to voids in aggregates filled with relatively finer materials or fouling agents that reduce the shear strength and lead to poor drainage (Huang *et al.* 2009, Li *et al.* 2015, Touqan *et al.* 2020); and (iv) differential settlement and shear failure that may occur on tracks built on highly compressible soft clays residing in low lying terrain, and with very low undrained shear strength.

With this increasing demand for freight trains in Australia, it would be inappropriate to operate heavy hauls on ballasted tracks built on formation soils without testing on large-scale sections of prototype model track. Since existing Australian railway design practices are mainly based on static loading conditions, they are only suited to shorter trains with low axle loads travelling at speeds of less than 80 km/h. In some parts of Australia, freight trains can be almost 4 km long, so the ballast degradation (breakage), mud pumping of certain formation soils, and differential settlements must be studied and quantified to achieve a resilient track design and avoid hefty maintenance costs after construction (Raymond and Bathurst 1994, Brown *et al.* 2007, Biabani *et al.* 2016, Ferreira and Indraratna 2018, Indraratna *et al.* 2018b, 2019, Powrie *et al.* 2019).

Conventional triaxial testing is a popular approach of evaluating the strength and breakage of ballast aggregates in the laboratory (Raymond and Davies 1978, McDowell *et al.* 2005, Brown *et al.* 2007, Aursudkij *et al.* 2009, Sevi *et al.* 2009, Zhang *et al*. 2017, Harkness *et al.* 2016, among others). However, the discrepancy between the actual shape and size of particles in the field and the much smaller particle sizes adopted in conventional laboratory equipment contributes to inaccurate load and deformation responses measured in the laboratory. Moreover, since the bottom boundary is rigid and is typically less than 600mm deep, this boundary condition cannot simulate the actual field track substructure. This means that testing coarse aggregates in conventional apparatus can yield misleading results due to the disparity in size between particle and equipment and the limited depth of subgrade (Lim *et al.* 2005, Peijun and Xubin 2007, Indraratna *et al.* 2018a). Previous large-scale triaxial tests carried out by many researchers have shown that the ratio between the size of the testing chamber and the particle size must be greater than 7-8 to reduce boundary effects (Marachi *et al.* 1972, Marsal 1973, Lade *et al.* 1996).

To alleviate these size dependent issues, examine a range of Australian ground conditions and integrated track components, the National Facility for Heavy-haul Railroad Testing (NFHRT) was the first to be designed and built in-house at Russell Vale, NSW, Australia. The NFHRT allows for a full size instrumented railway track section to be tested so that the effects of track substructure can be captured. Such a facility could not be established through purely commercial means; rather, it was designed and built in close cooperation with the Australian rail industry, a consortium of transport research centres in several Australian Universities and the Australian Research Council, c/o Ministry of Education, under the leadership of the first author.

In fact, the Australian rail industry has strongly promoted the state-of-the-art test facilities for heavy haul track modelling, and this was the main driver for constructing the first NFHRT under Commonwealth government funding channelled through the Australian Research Council. In particular, the NFHRT was designed and built in close cooperation with Australian Rail Track Corporation (ARTC) and Sydney Trains, whereby an array of typical ground conditions and integrated track components were considered in relation to the national flagship project Melbourne to Brisbane Inland Rail (MBIR), one of the longest heavy haul tracks to be completed soon.

Although similar test facilities have also been built in other countries (Brown *et al.* 2007, Bian *et al.* 2014, Abadi *et al.* 2016, Li *et al.* 2018, Bian *et al.* 2020, Hasnayn *et al.* 2020), these were built mainly for high-speed passenger trains capturing more favourable foundation characteristics in cold regions (e.g., stiff boulder clays and glacial tills) or for concrete slab tracks used for short high speed commuter trains (Zhang *et al.* 2019a, 2019b, Zhai *et al.* 2020, Li *et al.* 2020). Conversely, the Australian soft soil terrains for very long heavy axle freight trains are considerably different, including highly compressible black soils and deposits of upper Holocene soft clays. In this regard, the overall objective of the NFHRT is to contribute to innovative and more cost-effective designs for heavy haul tracks built on an array of problematic ground conditions.

It is noteworthy that the true moving load effect cannot be properly modelled using the NFHRT, as the cyclic loading is applied by four dynamic actuators in synchronized operation. This facility is mainly for simulating heavy haul ballast tracks for high axle freight trains that operate at low speeds. At high speeds exceeding say 130 km/h, there is significant principal stress rotation under moving loads, which cannot be simulated accurately by this facility as it only has two pairs of actuators. For simulating a true moving load at high speeds (exceeding say 130 km/h), one needs more than two pairs of actuators acting along a greater number of sleepers (Bian *et al.* 2014). In addition, the dynamic and impact effects due to track irregularities could not be captured in these model tests, and this is a limitation of the current study.

The main objective of this research is to introduce Australia's NFHRT that has recently been constructed and is now fully operational, as well as to validate the observed results against past field measurements available from heavy haul tracks located in the towns of Bulli and Singleton (NSW, Australia). The results of the first test are presented in this paper and compared with the available field monitoring data. These results will also serve as a benchmark for future tests considering varying track substructure conditions (e.g., excessive settlement of compressible soft soils and instability of saturated subgrade including mud-pumping), the effectiveness of artificial inclusions such as geosynthetics for improved track stability and the vibration mitigation of carriage-track-foundation interactions using damping elements made of recycled rubber. Details of the NFHRT, test set up, instrumentation, and the results of the first test are presented in the following sections.

2. National Facility for Heavy-haul Railroad Testing

2.1. Design and construction of the NFHRT

The NFHRT consists of a large-scale laboratory test facility that allows the testing of a fully instrumented ballasted track section at 1:1 prototype scale. It includes a test pit, loading frames, a hydraulic servo-controlled system with four dynamic actuators and a high capacity hydraulic power unit, an electrical system, an instrumentation and data acquisition system, and a 5-tonne overhead crane. A schematic of the NFHRT is shown in Figure 1a.

A 6.0m-long × 6.0m-wide × 2.3m-deep test pit was excavated, and four 900mm-thick reinforced concrete walls and a 600mm-thick reinforced concrete floor were then constructed (Fig. 1b). The hydraulic actuators and power unit of the NFHRT were designed, fabricated and then assembled (Fig. 1c). A trench for the hydraulic pipework (9.13m long × 1.35m wide × 0.5m high) was built with reinforced concrete walls (Fig. 1d).

Track materials such as ballast, capping, structural fills, subgrade, and a drainage layer are installed beneath a rail-sleeper assembly to accurately estimate their actual response when subjected to realistic loading conditions. A hybrid hydro-electrical substation with heavy duty hose connections from the hydraulic pipework to the four dynamic actuators provide the cyclic loading capable of simulating up to 40-tonne axle trains operating at speeds up to 200km/h. The actuators apply the designed cyclic loading directly onto the rails and are fully controlled through the computerised operating system also linked to an automated data acquisition system.

2.2. Materials and test procedures

In this first test, a 75mm thick drainage layer consisting of coarse grained gravel was placed at the bottom of the test pit (Fig. 2a) overlain by a geotextile filter to avoid clogging. A 795mm-thick layer of fine-grained subgrade soil (classified as CL according to the Unified Soil Classification System) was then installed and spread by a mini excavator. The subgrade was compacted in four sub-layers to a dry unit weight of 16.5 kN/m^3 (moisture content, w=20%) using a lightweight compaction plate. Pressure cells, soil moisture sensors and pore water pressure gauges were installed within the subgrade to measure the respective parameters during testing (Fig. 2b and 2d). An irrigation system consisting of a series of perforated pipes wrapped with a geotextile filter was installed in the subgrade layer to control the water content and the degree of saturation of the track foundation (Fig. 2c).

A 650mm-thick structural fill layer (moisture content, w=11.5%) was placed on top of the subgrade and compacted in sub-layers of 150 mm thick to achieve a dry unit weight of 18.5 kN/m^3, using similar procedures to those described earlier for the subgrade layer. A 180mm thick capping layer (sub-ballast) consisting of a sand and gravel mixture was then placed over the structural fill (Fig. 3a) and compacted in two sub-layers (90mm thick) to a dry unit weight of 19.5 kN/m^3, corresponding to about 90% of γ_{dmax} based on the standard Proctor compaction method in accordance with AS 1289.5.1.1 (2017). A heavier compaction plate was used to compact the sub-ballast material, giving the higher compaction requirements of this layer. To ensure all the materials from the bottom subgrade layer to the capping layer had been compacted to the desired unit weight, sand cone tests were conducted following the ASTM D1556 (2007) (Fig. 3b). Pressure cells and horizontal displacement transducers were then placed over the capping layer, as shown in Figure 3c.

Ballast (latite basalt aggregates) was obtained from the Bombo quarry, about 100km South of Sydney, then cleaned and sieved following the Australian Standards (AS 2758.7, 2015). The ballast was compacted in three sub-layers (100mm-thick) to achieve a density of nearly 16 kN/m^3 and the total thickness of the load-bearing ballast was 300mm, as typically used in actual Australian heavy-haul tracks (Fig. 3d). The selected densities for the track substructure layers are comparable with other studies reported earlier by Suiker *et al.* (2005), Aursudkij *et al.* (2009), Biabani *et al.* (2016) and Anderson and Fair (2008).

A system of rails and sleepers provided by the Australian Rail Track Corporation (ARTC) was laid onto the ballast layer (Fig. 3e) and additional ballast aggregates were then placed to simulate the crib and shoulder ballast. The loading frames were bolted in position and the four dynamic actuators were installed to apply a dynamic train loading (Fig. 3f). The particle size distribution (PSD) of the ballast, capping, structural fill and subgrade materials used for this test are shown in Figure 4.

2.3 Instrumentations

Figure 5a presents a plan view of the instrumentation installed into the track substructure such as settlement pegs (1-16), horizontal displacement transducers (E_{1T}, E_{1B}, E_{2T} and E_{2B}), pressure cells and the positions of the rail and sleeper system. Figure 5b is a cross section (North-South section) of the testing pit showing the locations of the sensors. Twenty rapid response hydraulic pressure cells were installed at different locations and depths to measure the transient vertical and horizontal stresses; sixteen settlement pegs were installed at varying depths in the structural fill, capping and ballast layers to measure the permanent vertical deformations. Four horizontal displacement transducers were placed bellow the loaded sleepers at two different depths (i.e., two of which were installed underneath the sleepers and the other two were installed at the bottom of the ballast layer). Two triaxial accelerometers were installed on the rail and sleeper to measure acceleration (vibration) during the tests (Fig. 6a). In addition, eight pore water pressure transducers, four moisture sensors and four water potential sensors were placed in the subgrade to monitor the excess pore pressure and/or the changes of water content and water potential, depending on the moisture conditions of the subgrade layer in each test. These sensors were installed in the subgrade layer for future tests considering the submergence of subgrade through the irrigation system to study track problems associated with flooded track conditions in low-lying coastal areas as well as the saturated subgrade instability, e.g., mud-pumping. Measurements from these sensors will be available for the future tests when the track substructure is made to be saturated. All the sensors and instruments were calibrated before testing. A data acquisition system controlled by a host computer automatically recorded all the data collected during the test (Fig. 6b). The selected sample rate (data logging frequency) for all the signals was 1200 Hz.

2.4 Cyclic loading characteristics

In this test, the load was selected based on a typical Australian freight train having an equivalent 25-tonne axle load. Therefore, a maximum load of 12.5 tonnes (125 kN) was applied by each dynamic actuator, simulating a realistic wheel load. The applied loading characteristics are schematically shown in Figure 7 corresponding to a vertical load of P_{max}=125 kN, P_{min}=15 kN and P_{mean}=70 kN, corroborating to a freight train of 25-tonne axle load. The minimum load of 15kN ensured continual contact between the dynamic actuators and the rails during the test.

The applied frequency of f=15 Hz in the experimental program is assumed to cover a realistic range of heavy haul train speeds of 60-80km/h on standard gauge tracks, based on Indraratna et al. (2011), Sun et al. (2016) and Navaratnarajah et al. (2018). In reality, the frequency is not only dependent on the train speed but also on track geometry, bogey spacing, rest periods, variations in cyclic and impact loading among other variables. For typical Australian freight train, the loading frequency was estimated by considering the distance between the last wheel of the front bogie and the first wheel of the next bogie on a standard gauge track in Australia. As the axle distance is much smaller than the length between bogie centers (L_b) or vehicle length, the two rear axles of a leading wagon and two front axles of a trailing wagon would represent the highest generated frequency (Indraratna *et al*. 2011). Heavy haul trains in Australia are often 4-5 km long and they travel on standard gauge tracks at relatively low speed (@ 40-60 km/h in most cases and rarely exceed 70k/h), and the applied frequency in the laboratory is indeed corroborated with the track geometry and train speed (e.g. Indraratna et al. 2011, Sun et al. 2016, Navaratnarajah et al. 2018). It is also noticed that there can be several variables including the sleeper spacing, speed of train, track irregularities, occasional impact loading, influence of rest periods, variation in cyclic loading due to non-uniform axle spacing etc. that can contribute to the real-life frequency in contrast to the simplified (constant) experimental magnitude of frequency.

The actuators worked in synchronised pattern up to N=500,000 load cycles to simulate the realistic repeated loading on the rails, but given the limitation of having only two pairs of actuators, the ideal simulation of moving loads from the bogies of a long train was not possible. As mentioned earlier, the design of this equipment is reasonable for slow moving heavy haul trains in Australia, but not for representing high speed passenger trains where significant principal stress rotation occurs under fast moving loads. In addition, it is noted that the loading sequence capturing rest periods is not considered in this study. This is because the worst conditions occur when very long heavy haul trains apply continual loading over a substantial period of time, and busy freight tracks in the mining hubs have relatively small rest periods. For example in Western Australia, different mineral ore trains can travel over very long distances at slow speeds (40-60 km/h) from source to port (sometimes up to 300 km) regularly most of the day, and the ballast relaxation during relatively short rest periods between these slow-moving trains can be ignored. For instance, for iron ore trains that can be up to 6 km long moving at only 40 km/h, the worst-case scenario simulated in the laboratory is without any rest period, so that the fatigue of ballast is maximised during testing to determine the maximum deformation, i.e. settlement and lateral movement. Both the axle load and loading frequency influence the resulting settlement, but the axle load magnitude is more dominant than the frequency. Nevertheless, the load frequency must still be highlighted, because that is the only loading parameter in cyclic laboratory testing that is related to the train speed (Esveld, 2014; Indraratna et al. 2011). In other words, the number of axle loads passing through a specific in situ reference point (worksite) over a given period of time is related to the frequency.

3. Results and discussion

3.1. Measured vertical settlement

Figure 8 shows the accumulated track settlement after being subjected to a 25-tonne axle load at a frequency of f=15 Hz, as recorded by the settlement pegs installed below the sleepers (S_1, S_5, S_{10} and S_{16} – Fig. 5a). It can be concluded that the vertical displacement (S_v) of ballast increased rapidly up to about N=50,000 cycles due to its initial densification and subsequent packing as the corners of the sharp angular ballast aggregates began to break (S_v = 6.2 mm to 8.7 mm). However, once the aggregates began to stabilise the rate of vertical displacement gradually decreased and remained relatively constant after N=200,000 cycles (S_v = 8.7 mm to 12.1 mm). This shows the aggregate density has reached threshold compression and would resist further rearrangement and densification with additional cycles. The measured final track settlement, taking the average of the four settlement pegs, was about S_v=14.2 mm. These observations are in agreement with the data obtained in the laboratory (Indraratna *et al.* 2013) and the field measurements taken at the Bulli and Singleton tracks (Indraratna *et al.* 2010, 2014). It is noted that while the track settlement measured at the Bulli track matched those measured at the NFHRT facility, field data from the Singleton track showed higher vertical settlement, especially after N=200,000 cycles. This could be due to the track section at Singleton being built on a flood plain with a 7-10 m thick layer of alluvial silty clay, which could lead to greater vertical deformation of the track.

3.2. Measured lateral displacement

Figure 9 presents the lateral displacement (S_h) of the ballast layer as recorded by the four horizontal displacement transducers, two of which (E_{1T}, E_{2T}) were placed underneath the sleepers and the other two (E_{1B}, E_{2B}) were installed at the boundary between the ballast and capping layers at the bottom of the ballast layer (Fig. 5). The lateral displacement of ballast measured at the Bulli track and from laboratory tests performed earlier (Indraratna *et al.* 2010, 2013) are also shown in Figure 9 for comparison purposes. The measurements from all the displacement transducers show consistent increases in lateral displacement with increased N. The ballast aggregates showed a significant horizontal spread (S_h=5.8 mm - 6.2 mm) within the initial N=100,000 cycles, followed by a gradual increase in S_h up to N=300,000 cycles, after which S_h remained nearly constant towards the end of the test. The final horizontal displacement of the track varied from S_h=6.8 mm - 9.1mm, depending on the location of each measurement. This trend is similar to those observed earlier in actual rail tracks and in the laboratory by Indraratna *et al.* (2013). However, the data from the field trial at Bulli track show higher lateral displacements than those measured at the NFHRT. This is possibly because moving freight trains generate greater impact forces due to wheel or rail irregularities such as flat wheels, dipped rails, expansion gaps and rail corrugations, which could accelerate the degradation and lateral spreading of ballast (Auersch 2015, Ferreira and Indraratna 2018, Indraratna *et al.* 2020a). Furthermore, in the NFHRT two aluminium panels (200mm-high) were placed on both sides of the shoulder ballast to maintain track geometry during the commissioning process, which may have provided some additional confinement to the ballast layer leading to slightly lower lateral deformations when compared to the field measurements at Bulli track.

3.3. The vertical and lateral stresses

Figure 10a shows the typical vertical stresses recorded over time at different depths of the track substructure (from the top surface of the ballast to the drainage layer) during the test. Pressure cells were placed between the sleepers and ballast, beneath the ballast layer, between the capping and structural fill, and on top of the subgrade and drainage layers to measure the stresses at different depths (Fig. 5b). Under a 25-tonne axle load the maximum vertical stress at the sleeper-ballast interface is about σ_v = 225 kPa, and the σ_v attenuates with depth. The maximum vertical stresses at the top surface of the capping layer, the structural fill, the subgrade and drainage layers are measured as σ_v = 151, 132, 98, and 54 kPa, respectively. The vertical stresses at different depths plotted on the frequency domain are shown in Figure 10b. Here, the cyclic response of the stresses recorded in the ballast layer peaks at f=15Hz, but these peaks decrease slightly in the underlying layers showing how the loading frequency attenuates with depth.

Figure 11 illustrates the vertical stress (σ_v) measured at different layers of the track substructure and its variation with the number of load cycles. It is evident that the dynamically induced stress in the ballast layer increases with N (e.g., at the first N=500 cycles, σ_v =175 kPa, and then σ_v continues to increase to σ_v =225 kPa at the end of the test, N=500,000 cycles). On the other hand, the vertical stress σ_v decreases with the depth of the test pit where the σ_v recorded in the subgrade and drainage layers is approximately 95 kPa and 48 kPa, respectively. The vertical stresses obtained in a previous laboratory study and on the field tracks (Singleton and Bulli tracks) are also plotted in Figure 11 for comparison purposes (Indraratna *et al.* 2010, 2014, Navaratnarajah *et al.* 2018). Given that the laboratory equipment used in the previous study has a limited boundary, only the stresses up to a depth of 500 mm below the surface of ballast are presented. The σ_v reported in previous studies shows some fluctuations where σ_v between the sleeper and ballast varies from 172 kPa to 300 kPa, and then decreases to about 38 kPa (Bulli track) and 87 kPa (laboratory test) when measured at the top surface of the capping layer.

Figure 12 shows the horizontal stresses (σ_h) in the ballast layer obtained in the longitudinal direction parallel to the rails and in the transverse direction parallel to the sleepers. Data were monitored by two pressure cells placed at the northern and southern sides of the track (lateral confinement in the transverse direction - σ_3) and two pressure cells placed on the eastern and western walls to measure the longitudinal stresses (σ_2). It is seen that the horizontal stress (σ_h) remains almost unchanged during the test. Lateral confinement in the transverse direction, commonly known as the confining pressure (σ_3), is around σ_3=22 kPa to 25 kPa during the test, whereas the longitudinal stress (the intermediate stress, σ_2) varies from σ_2=15 kPa to 20 kPa. The lateral stresses in the transverse direction exceeded those in the longitudinal direction possibly because the latter were measured by pressure cells fixed to the vertical steel walls, which were further away from the locations of load application (actuators). The confining pressures measured in this study are generally consistent with those recorded during previous field monitoring programmes carried out in Australian heavy-haul tracks.

3.4. Measured resilient modulus

The resilient modulus (M_R) of ballast can be calculated as the ratio between the deviatoric stress (Δ_{qcyc}) and the resilient (recoverable) axial strain ($\varepsilon_{a,rec}$) during loading-unloading stage, as given by:

$$M_R = \frac{\Delta q_{cyc}}{\varepsilon_{a,rec}} = \frac{q_{cyc,max} - q_{cyc,min}}{\varepsilon_{a,rec}} \tag{1}$$

The resilient (recoverable) axial strain ($\varepsilon_{a,rec}$) was obtained at a given number of loading–unloading cycles (N) using the data bursting approach to determine the resilient modulus (M_R) of ballast. During the test, the relevant sets of data bursting were initiated at N= 1, 50, 100, 500, 1000, 5000, 10,000, 50,000, 100,000, 200,000, 300,000, 400,000, and 500,000; and the recoverable axial strains ($\varepsilon_{a,rec}$) during unloading were determined by subtracting the measured axial strains of the corresponding loading-unloading cycle. Figure 13a shows the typical stress-strain hysteresis loops plotted for a given load cycle. It can be observed that the areas of the hysteresis loops are reduced as the number of load cycles (N) increases, which indicates that ballast aggregates become more compacted and respond more elastically with increased N. The variation of resilient modulus M_R with N presented in Figure 13b shows a rapid increase of M_R within the first N = 200,000 cycles (M_R=462 MPa), after which the rate at which M_R increased becomes marginal. The rapid compression and densification of ballast during the initial load cycles increases track stiffness, leading to a rapid increase in M_R at the beginning of the test. After N=200,000 loading cycles the ballast aggregates may move to the shakedown stage, which causes the M_r to remain relatively unchanged (Le Pen *et al.* 2016, Sun *et al.* 2019).

3.5. Rail and sleeper acceleration

As mentioned, two triaxial accelerometers (A_R and A_S) were installed on the rail and sleeper to measure acceleration (vibration) during the tests. The acceleration of the rail and sleeper plotted in time and frequency domains are shown in Figure 14. Here, the accelerations measured at the sleeper (A_S) are greater than those recorded at the rail (A_R), with a maximum value of A_s = 27.2 m/s^2 compared to the highest value of A_R = 5.6 m/s^2. It is noteworthy that the rails were connected to six concrete sleepers creating a stronger system that could prevent from excessive vertical vibration, while the edge of sleeper was more prone to vertical displacement due to sitting on the discrete ballast aggregates. The accelerations were measured at the end of the test where the ballast shoulder has significantly displaced laterally and could cause the condition of hanging sleeper. As a result, there was a reduction in lateral confinement applied to the sleepers that resulted in increased sleeper displacement and associated acceleration.

The acceleration (vibration) in the time domain is converted into the frequency domain by the fast Fourier transform (FFT), as shown in Figure 14. It is observed that the responses reach their maximum peak values at an approximate frequency of f_1 = 15 Hz, while some smaller peaks are reached at higher frequencies (Kouroussis *et al.* 2009). The f_1 frequency is identical to the cyclic loading applied by the dynamic actuators, which indicates that the response of the track substructure to acceleration is in the same phase as the applied loading frequency.

3.6. Measured ballast breakage

After the test, ballast aggregates at four different locations (underneath two actuators, between the two rails, and at the shoulder ballast) were recovered separately for quantifying ballast breakage. This ballast was then passed through standard sieves to obtain the particle size distribution (PSD), as shown in Figure 15. Indraratna *et al*. (2005) introduced a new method to quantify ballast degradation under cyclic loading, which leads the PSD curve of ballast to shift towards the smaller size particles due to breakage. By recognising this shift as the degradation indicator, the ballast breakage index (*BBI*) can be calculated using Equation 2

$$BBI = \frac{A}{A+B} \qquad (2)$$

where, *A* is the shift in PSD due to ballast breakage under cyclic loading, and *B* is the potential breakage or the area between the arbitrary boundary of maximum breakage and the final particle size distribution. It is noted the upper and lower limits of *BBI* are 0 (no breakage) and 1, respectively. A summary of the sieve analysis performed before and after the test for quantifying ballast breakage (*BBI*) is presented in Table 1. Measured breakage denotes that ballast aggregates collected directly underneath the actuators had the highest amount of breakage, estimated as $BBI_{1,2}$ = 0.143 and 0.115, whereas the ballast collected from between two rails (crib ballast) and the edge of a sleeper (shoulder ballast) have $BBI_{3,4}$ = 0.085 and 0.075, respectively. The ballast underneath the actuators experiences more breakage because these aggregates carry the cyclic loads directly from the dynamic actuators and also deal with the vibration transferred from the sleepers. As a consequence, these aggregates are more prone to breakage. The results also show that the average *BBI* for ballast samples collected underneath the actuators (*BBI* = 0.129) was slightly higher than that obtained for ballast aggregates recovered from beneath the sleeper and rail seat in the actual heavy-haul track at Singleton after the same number of load cycles (Nimbalkar and Indraratna 2016). In fact, in the NFHRT the load is continually applied over the same sleepers for 500,000 cycles, which results in a slightly higher amount of ballast crushing when compared to actual field measurements.

4. Conclusions

This paper described the construction and testing process of the new Australia's National Facility for Heavy-haul Railroad Testing (NFHRT), a prototype test facility that allowed investigating the performance of a real-size instrumented track section when subjected to continuous cyclic loading applied via two pairs of dynamic actuators. The first test was carried out under a 25-tonne axle load applied at a frequency of 15 Hz to cover a realistic range of heavy haul train speeds of 60-80km/h on standard gauge tracks. The results from this first test, including the measured track settlement and lateral deformation, transient vertical and lateral stresses, rail and sleeper accelerations, resilient modulus and breakage of ballast were presented and compared with actual field measurements obtained in heavy-haul tracks located in the towns of Bulli and Singleton (New South Wales, Australia).

The obtained results were generally consistent with real-life measurements undertaken during the aforementioned field monitoring programmes. An average track settlement of about 14 mm and lateral deformations up to 9 mm were recorded after 500,000 load cycles. Any small discrepancies between the test results and the actual field measurements may be associated with boundary conditions and loading simulations. For instance, the lateral deformation of the ballast layer recorded in the field trial conducted at Bulli exceeded that measured in the NFHRT. This is partially because moving freight trains generate greater impact forces due to wheel or rail irregularities, which could accelerate the lateral spreading of ballast. On the other hand, the breakage of the load-bearing ballast estimated at the end of the test (*BBI* = 0.129) was found to be slightly higher than that measured in the actual rail track at Singleton, which can be related to the fact that in the NFHRT the load was continually applied over the same sleepers for 500,000 cycles, thus resulting in a higher extent of ballast degradation.

It is noteworthy that the true moving load effect was not properly modelled in the test reported herein, as the cyclic loading was applied by four dynamic actuators in synchronized operation. In spite of this limitation, the obtained results for these relatively low speeds (≈ 60-80 km/h) were acceptable as the facility mimicked the cyclic loading appropriately. However, at very high speeds the results may deviate from accuracy when fast moving loads must be simulated correctly with more than two pairs of actuators acting along a greater number of sleepers (Bian *et al*. 2014).

When compared to smaller-scale or conventional laboratory test facilities, the NFHRT enabled to mitigate boundary effects and more realistically simulate Australian track conditions (often involving problematic subsoils) in a controlled laboratory environment. The test reported in this paper was aimed at simulating the conditions prevailing in typical Australian heavy-haul tracks. Additional tests will be carried out in the future to examine the benefits of artificial inclusions, such as geosynthetics and recycled rubber products, as well as the influence of different substructure materials (including recycled waste materials) on track performance, which will facilitate innovative and more sustainable designs for enhanced stability and resiliency of heavy haul tracks.

Acknowledgements

This study was carried out by the ARC Industrial Transformation Training Centre for Advanced Technologies in Rail Track Infrastructure (ITTC-Rail) and was funded by the Australian Government (IC170100006). The financial support from the Australian Research Council through the Linkage Infrastructure, Equipment and Facilities scheme (LE140100010) is gratefully acknowledged. The authors also appreciate the insightful collaboration and assistance of Australian Rail Track Corporation (ARTC), Sydney Trains, Australasian Centre for Rail Innovation (ACRI), SMEC, RM CRC, among others, for their continuous cooperation and support. The authors are also grateful to UOW's technical staff, namely, Mr Alan Grant, Mr Duncan Best, Mr Cameron Neilson, and Mr Ritchie McLean for their assistance during the construction and commissioning of the NFHRT.

References

Abadi, T., L. Le Pen, A. Zervos and W. Powrie (2016). A Review and Evaluation of Ballast Settlement Models using Results from the Southampton Railway Testing Facility (SRTF). Procedia Engineering 143: 999-1006.

AS 2758.7 (2015). Aggregates and rock for engineering purposes, Part 7. Railway Ballast. Standards Australia, NSW, Australia.

AS 1289.5.1.1 (2017). Methods of testing soils for engineering purposes, Method 5.1.1: Soil compaction and density tests - Determination of the dry density/moisture content relation of a soil using standard compactive effort. Standards Australia, NSW, Australia.

ASTM D1556 (2007). Standard test method for density and unit weight of soil in place by the sand-cone method. ASTM International, West Conshohocken, PA, USA.

Anderson, W.F., and Fair, P. (2008). Behavior of railroad ballast under monotonic and cyclic loading. Journal of Geotechnical and Geoenvironmental Engineering 143(3): 316–327.

Auersch, L. (2015). Force and ground vibration reduction of railway tracks with elastic elements. *Journal of Vibration and Control*, **21**(11), 2246-2258.

Aursudkij, B., McDowell, G.R. and Collop, A.C. (2009). Cyclic loading of railway ballast under triaxial conditions and in a railway test facility. *Granular Matter*, **11**, 391–401.

Biabani, M.M., Ngo, N.T. and Indraratna, B. (2016). Performance evaluation of railway subballast stabilised with geocell based on pull-out testing. *Geotextiles and Geomembranes*, **44**(4), 579-591.

Bian, X., H. Jiang, C. Cheng, Y. Chen, R. Chen and J. Jiang (2014). Full-scale model testing on a ballastless high-speed railway under simulated train moving loads. Soil Dynamics and Earthquake Engineering 66: 368-384.

Bian, X., Gao, Y., Huang, H., and Xie, Y. (2017). Hanging tie study using the “moving deflection spectrum”. Proceedings of the Institution of Mechanical Engineers, Part F: Journal of Rail and Rapid Transit, 231(8): 982-990.

Bian, X., Li, W., Qian, Y. and Tutumluer, E. (2020). Analysing the effect of principal stress rotation on railway track settlement by discrete element method. *Géotechnique*, **0**(0), 1-19.

Brown, S.F., Brodrick, B.V., Thom, N.H. and McDowell, G.R. (2007). The Nottingham railway test facility, UK. *Proceedings of the Institution of Civil Engineers - Transport*, **160**(2), 59-65.

Brown, S.F., Kwan, J. and Thom, N.H. (2007). Identifying the key parameters that influence geogrid reinforcement of railway ballast. *Geotextiles and Geomembranes*, **25**(6), 326-335.

Budiono, D.S., McSweeney, T., Dhanasekar, M. and Gurung, N. (2004). "The effect of coal dust fouling on the cyclic behaviour of railtrack ballast." *Cyclic Behaviour of Soils and Liquefaction phenomena*, Taylor & Francis Group, London.

Cai, Y., L. Xu, W. Liu, Y. Shang, N. Su and D. Feng (2020). Field Test Study on the dynamic response of the cement-improved expansive soil subgrade of a heavy-haul railway. Soil Dynamics and Earthquake Engineering, 128: 105878.

Esveld, C. (2014). Modern railway track, MRT Press, The Netherlands.

Ferreira, F. and Indraratna, B. (2018). Deformation and degradation response of railway ballast under impact loading–effect of artificial inclusions. In ICRT 2017: Railway Development, Operations, and Maintenance - Proceedings of the 1st International Conference on Rail Transportation, p. 1090-1101.

Guo, Y., Fu, H., Qian, Y., Markine, V. and Jing, G. (2020). Effect of sleeper bottom texture on lateral resistance with discrete element modelling. *Construction and Building Materials,* **250**, 118770.

Harkness, J., Zervos, A., Le Pen, L., Aingaran, S. and Powrie, W. (2016). Discrete element simulation of railway ballast: modelling cell pressure effects in triaxial tests. *Granular Matter,* **18**(3), 65.

Hasnayn, M.M., McCarter, W.J., Woodward, P.K. and Connolly, D.P. (2020). Railway subgrade performance after repeated flooding–Large-scale laboratory testing. Transportation Geotechnics, 23, p.100329.

Huang, H., Tutumluer, E. and Dombrow, W. (2009). "Laboratory characterisation of fouled railroad ballast behavior." *Transportation Research Record: Journal of the Transportation Research Board, No. 2117*, Washington, DC.

Hu, P., Zhang, C., Wen, S., and Wang, Y. (2019). Dynamic responses of high-speed railway transition zone with various subgrade fillings. Computers and Geotechnics, 108: 17-26.

Indraratna, B., Salim, W., & Rujikiatkamjorn, C. (2011). Advanced Rail Geotechnology - Ballasted Track: CRC Press, Taylor & Francis Group, London, UK.

Indraratna, B., Ferreira, F.B., Qi, Y. and Ngo, T.N. (2018b). Application of geoinclusions for sustainable rail infrastructure under increased axle loads and higher speeds. *Innovative Infrastructure Solutions*, **3**(1), 69.

Indraratna, B., Lackenby, J. and Christie, D. (2005). Effect of confining pressure on the degradation of ballast under cyclic loading. *Géotechnique,* **55**(4), 325–328.

Indraratna, B., Ngo, N.T., Ferreira, F.B., Rujikiatkamjorn, C. and Shahkolahi, A. (2020a). Laboratory examination of ballast deformation and degradation under impact loads with synthetic inclusions. *Transportation Geotechnics,* **25**, 100406.

Indraratna, B., Ngo, N.T., Nimbalkar, S. and Rujikiatkamjorn, C. (2018a). Two Decades of Advancement in Process Simulation Testing of Ballast Strength, Deformation, and Degradation. ASTM-Railroad Ballast Testing and Properties. **1605:** 11-38.

Indraratna, B., Ngo, N.T. and Rujikiatkamjorn, C. (2013). Deformation of coal fouled ballast stabilized with geogrid under cyclic load. *Journal of Geotechnical and Geoenvironmental Engineering*, **139**(8), 1275-1289.

Indraratna, B. and Ngo, T. (2018). Ballast Railroad Design: Smart-Uow Approach, CRC Press.

Indraratna, B., Nimbalkar, S., Christie, D., Rujikiatkamjorn, C. and Vinod, J.S. (2010). Field assessment of the performance of a ballasted rail track with and without geosynthetics. *Journal of Geotechnical and Geoenvironmental Engineering*, **136**(7), 907–917.

Indraratna, B., Nimbalkar, S. and Neville, T. (2014). Performance assessment of reinforced ballasted rail track. *Proceedings of the Institution of Civil Engineers - Ground Improvement*, **167**(1), 24-34.

Indraratna, B., Nimbalkar, S.S., Ngo, N.T. and Neville, T. (2016). Performance improvement of rail track substructure using artificial inclusions: Experimental and numerical studies. *Transportation Geotechnics*, **8**, 69-85.

Indraratna, B., Qi, Y., Ngo, T.N., Rujikiatkamjorn, C., Neville, T., Ferreira, F.B. and Shahkolahi, A. (2019). Use of geogrids and recycled rubber in railroad infrastructure for enhanced performance. *Geosciences*, **9**(1).

Indraratna, B., Singh, M., Nguyen, T.T., Leroueil, S., Abeywickrama, A., Kelly, R. and Neville, T. (2020b). A laboratory study on fluidization of subgrade under cyclic train loading. *Canadian Geotechnical Journal*.

Kouroussis, G., Verlinden, O. and Conti, C. (2009). Ground propagation of vibrations from railway vehicles using a finite/infinite-element model of the soil. *Proceedings of the Institution of Mechanical Engineers, Part F: Journal of Rail and Rapid Transit*, **223**(4), 405-413.

Lade, P.V., Yamamuro, J.A. and Bopp, P.A. (1996). Significance of particle crushing in granular materials. *Journal of Geotechnical Engineering, ASCE*, **122**(4), 309-316.

Le Pen, L., Milne, D., Thompson, D. and Powrie, W. (2016). Evaluating railway track support stiffness from trackside measurements in the absence of wheel load data. *Canadian Geotechnical Journal*, **53**(7), 1156-1166.

Li, D., Hyslip, J., Sussmann, T. and Chrismer, S. (2015). Railway geotechnics, CRC Press.

Li, W., X. Bian, X. Duan and E. Tutumluer (2018). Full-Scale Model Testing on Ballasted High-Speed Railway: Dynamic Responses and Accumulated Settlements. Transportation Research Record 2672(10): 125-135.

Li, H., Z. Wang, F. Huang, Z. Yi, Y. Xie, D. Sun and R. Sun (2020). Impact of different lithological manufactured sands on high-speed railway box girder concrete. Construction and Building Materials, 230: 116943.

Lim, W.L., McDowell, G.R. and Collop, A.C. (2005). Quantifying the relative strengths of railway ballasts. *Geotechnical Engineering*, **158**(2), 107–111.

Marachi, N.D., Chan, C.K. and Seed, H.B. (1972). Evaluation of properties of rockfill materials. *Soil Mechanics and Foundations Division: Proceedings of the American Society of Civil Engineers,* **98**(SM1), 95-115.

Marsal, R.J. (1973). Mechanical properties of Rockfill. In : Embankment Dam Engineering Wiley, New York, pp: 109-200.

McDowell, G.R., Lim, W.L., Collop, A.C., Armitage, R. and Thom, N.H. (2005). Laboratory simulation of train loading and tamping on ballast. *Proceedings of the Institution of Civil Engineers: Transport,* **158**(TR2), 89-95.

Mishra, D., Qian,Y., Huang, H. and Tutumluer, E. (2014). An integrated approach to dynamic analysis of railroad track transitions behavior. Transportation Geotechnics 1(4): 188-200.

Navaratnarajah, S.K., Indraratna, B. and Ngo, N.T. (2018). Influence of Under Sleeper Pads on Ballast Behavior Under Cyclic Loading: Experimental and Numerical Studies. *Journal of Geotechnical and Geoenvironmental Engineering,* **144**(9), 04018068.

Nimbalkar, S. and Indraratna, B. (2016). Improved performance of ballasted rail track using geosynthetics and rubber shockmat. *Journal of Geotechnical and Geoenvironmental Engineering* **142**(8), 04016031.

Paixão, A., Fortunato, E. and Calçada (2016). A numerical study on the influence of backfill settlements in the train/track interaction at transition zones to railway bridges. Proceedings of the Institution of Mechanical Engineers, Part F: Journal of Rail and Rapid Transit ,230(3): 866-878.

Peijun, G. and Xubin, S. (2007). Shear strength, interparticle locking, and dilatancy of granular materials. *Canadian Geotechnical Journal,* **44**(5), 579.

Powrie, W., Le Pen, L., Milne, D. and Thompson, D. (2019). Train loading effects in railway geotechnical engineering: Ground response, analysis, measurement and interpretation. *Transportation Geotechnics,* **21**, 100261.

Powrie, W., Yang, L.A. and Clayton, C.R.I. (2007). Stress changes in the ground below ballasted railway track during train passage. *Proceedings of the Institution of Mechanical Engineers: Part F: Journal of Rail and Rapid Transit*, 247-261.

Priest, J.A., Powrie, W., Yang, L., Grabe, P.J. and Clayton, C.R.I. (2010). Measurements of transient ground movements below a ballasted railway line. *Geotechnique,* **60**(9), 667–677.

Raymond, G.P. and Bathurst, R.J. (1994). Repeated-load response of aggregates in relation to track quality index. *Canadian Geotechnical Journal,* **31**, 547-554.

Raymond, G.P. and Davies, J.R. (1978). Triaxial tests on dolomite railroad ballast. *Jounal of the Geotechnical Engineering Division: Proceedings of the American Society of Civil Engineers,* **104**(GT6), 737-751.

Sayeed, M.A. and Shahin, M.A. (2016). Three-dimensional numerical modelling of ballasted railway track foundations for high-speed trains with special reference to critical speed. *Transportation Geotechnics,* **6**, 55-65.

Sayeed, M.A. and Shahin, M.A. (2017). Design of ballasted railway track foundations using numerical modelling. Part I: Development. *Canadian Geotechnical Journal*, **55**(3), 353-368.

Selig, E.T. and Waters, J.M. (1994). Track geotechnology and substructure management, Thomas Telford, London.

Sevi, A., Ge, L. and Take, W. (2009). A Large-Scale Triaxial Apparatus for Prototype Railroad Ballast Testing. *Geotechnical Testing Journal,* **32**(4), 297-304.

Sol-Sánchez, M., F. Moreno-Navarro, R. Tauste-Martínez, L. Saiz and M. C. Rubio-Gámez (2020). Recycling Tire-Derived Aggregate as elastic particles under railway sleepers: Impact on track lateral resistance and durability. Journal of Cleaner Production, 277: 123322.

Suiker, A.S.J. and Borst, R. (2003). A numerical model for the cyclic deterioration of railway tracks. *International Journal for Numerical methods in Engineering*, **57**, 441–470.

Suiker, A.S.J., Selig, E.T., and Frenkel, R. (2005). Static and cyclic triaxial testing of ballast and subballast. Journal of Geotechnical and Geoenvironmental Engineering, 131(6): 771–782.

Sun, Q., Indraratna, B. and Ngo, N.T. (2019). Effect of increase in load and frequency on the resilience of railway ballast. *Géotechnique,* **69**(9), 833-840.

Sun, Q. D., B. Indraratna and S. Nimbalkar (2016). Deformation and Degradation Mechanisms of Railway Ballast under High Frequency Cyclic Loading. Journal of Geotechnical and Geoenvironmental Engineering, 142(1): 04015056.

Touqan, M., A. Ahmed, H. El Naggar and T. Stark (2020). Static and cyclic characterization of fouled railroad sub-ballast layer behaviour. Soil Dynamics and Earthquake Engineering, 137: 106293.

Wang, T., Luo, Q., Liu, M., Wang, L. and Qi, W. (2020). Physical modeling of train-induced mud pumping in substructure beneath ballastless slab track. *Transportation Geotechnics*, **23**, 100332.

Zhai, W.M., Wang, K.Y. and Lin, l.H. (2004). Modelling and experiment of railwayballast vibrations. *Journal of Sound and Vibration*, **673–683**, 673–683.

Zhai, W., Wang, K., Chen, Z., Zhu, S., Cai, C. and Liu, G. (2020). Full-scale multi-functional test platform for investigating mechanical performance of track-subgrade systems of high-speed railways. Railway Engineering Science, 28(3): 213-231.

Zhang, X., C. Zhao and W. Zhai (2017). Dynamic behavior analysis of high-speed railway ballast under moving vehicle loads using discrete element method." International Journal of Geomechanics 17(7): 04016157.

Zhang, X., Zhao, C., Zhai, W. and Shi, C. (2019a). Investigation of track settlement and ballast degradation in the high-speed railway using a full-scale laboratory test. Proceedings of the Institution of Mechanical Engineers, Part F: Journal of Rail and Rapid Transit, 233(8): 869-881.

Zhang, X., C. Zhao and W. Zhai (2019b). Importance of load frequency in applying cyclic loads to investigate ballast deformation under high-speed train loads. Soil Dynamics and Earthquake

Engineering 120: 28-38.

Table 1. Quantification of ballast breakage (*BBI*) recovered at different places after the test

Sieve size (mm)	**Passing (%)**				
	Initial gradation of tested ballast	Collected ballast underneath the South-East actuator	Collected ballast underneath the North-West actuator	Collected ballast between two rails	Collected ballast at the end of sleeper (shoulder ballast)
63	100	100	100	100	100
53	93.75	94.2	94.50	94.2	93.9
37.5	51.70	63.5	61.20	56.2	55.7
26.5	21.38	31.4	31.20	27.9	27.2
19	5.92	10.9	10.53	10.36	9.8
13.2	2.68	8.5	7.47	6.98	6.52
9.5	2.15	6.12	5.67	4.78	4.25
4.75	1.83	3.12	3.73	3.14	2.04
2.36	0	0	0	0	0
	Measured *BBI*	**0.143**	**0.115**	**0.085**	**0.074**

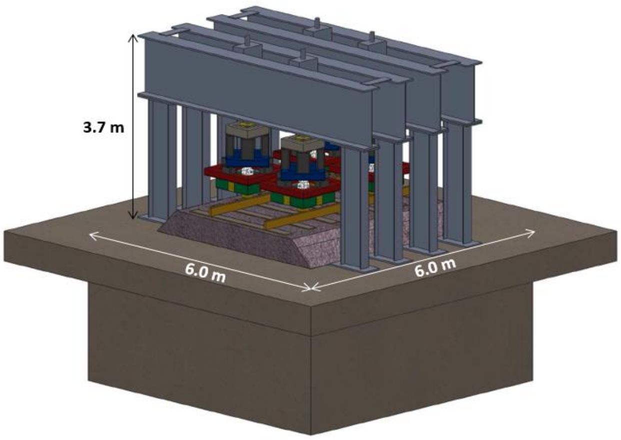

(a) Design concept

(b) Reinforced concrete of the test pit

(c) Hydraulic power unit

(d) Hydraulic pipe system

Figure 1. Design and construction of the NFHRT

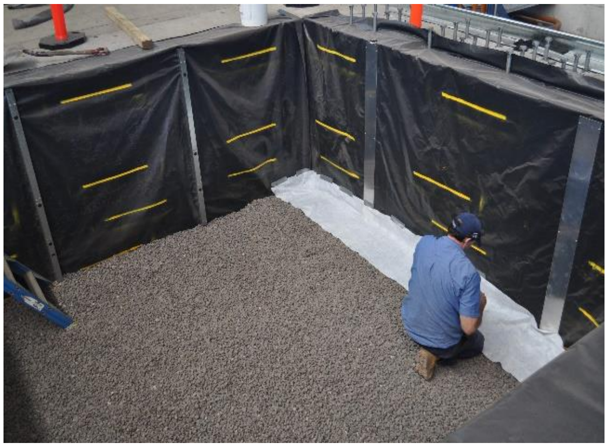

(a) Drainage layer

(b) Moisture sensors and pore pressure gauges

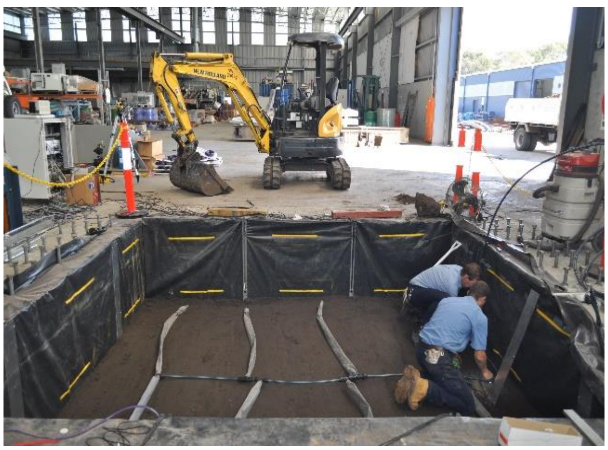

(c) Irrigation system

(d) Pressure cells on top of subgrade

Figure 2. Installation of the drainage and subgrade layers

(a) Capping layer

(b) Sand-cone test for compacted capping

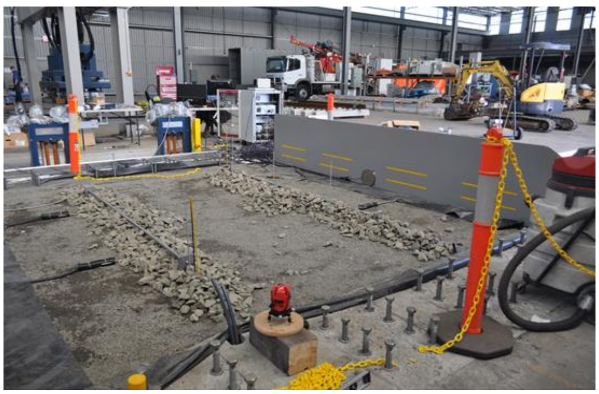

(c) Placement of ballast

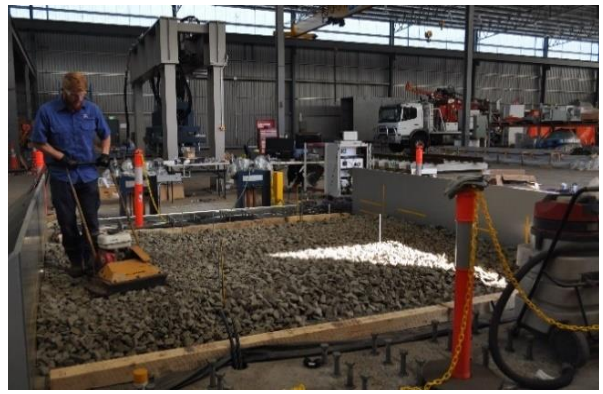

(d) Compaction of ballast layer

(e) Rails and sleepers

(f) Loading frames and hydraulic actuators

Figure 3. Installation of the capping, ballast, rail-sleeper assembly and dynamic actuators

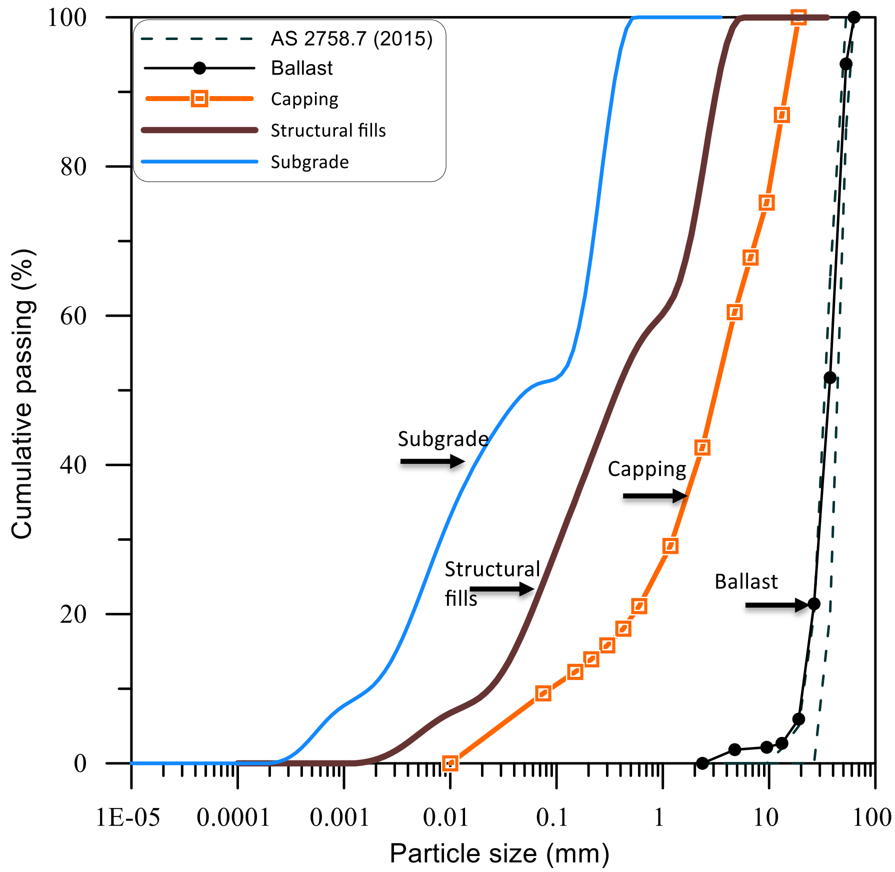

Figure 4. Particle size distribution curves of the track substructure materials

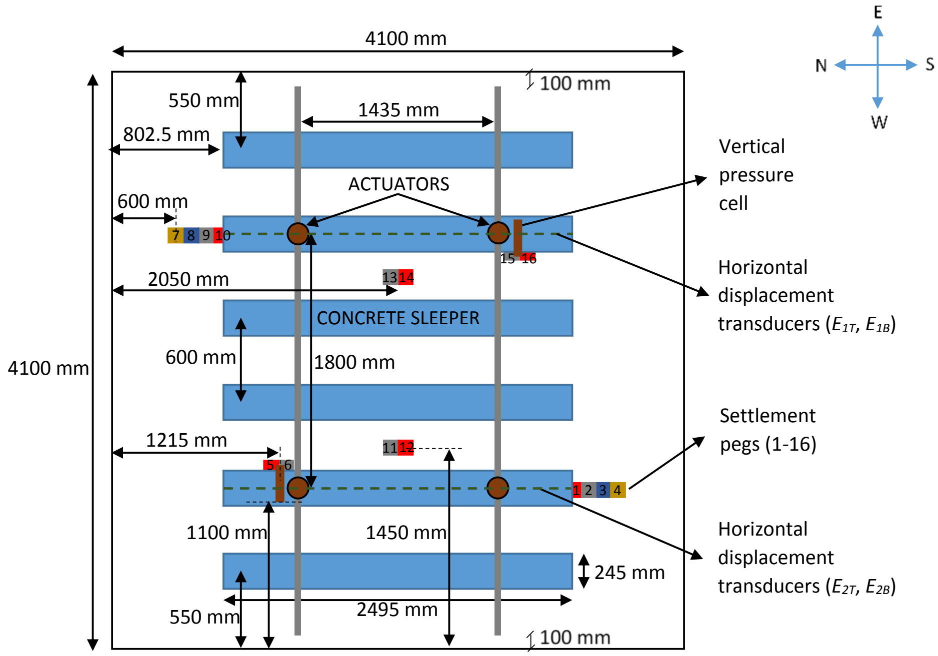

(a) Plan view of locations of instrumentations

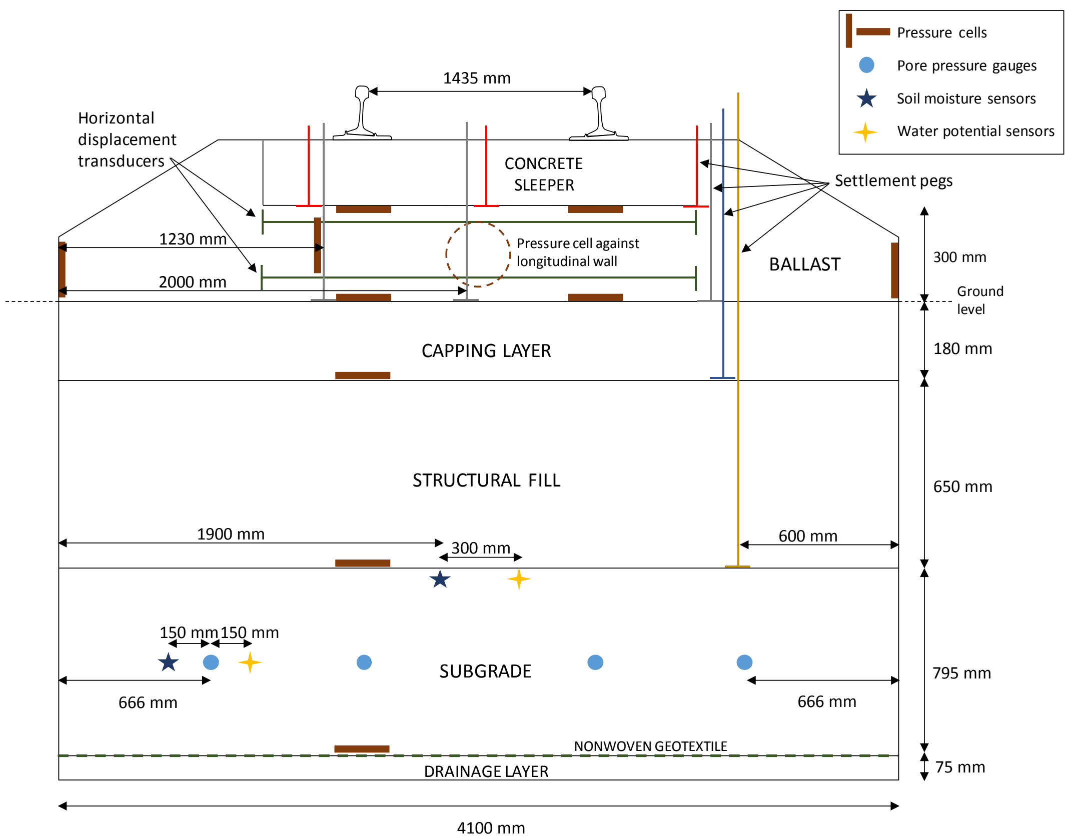

(b) A cross-section of the test pit with detailed instrumentations

Figure 5. A plan view and cross-section of the NFHRT with detailed instrumentations

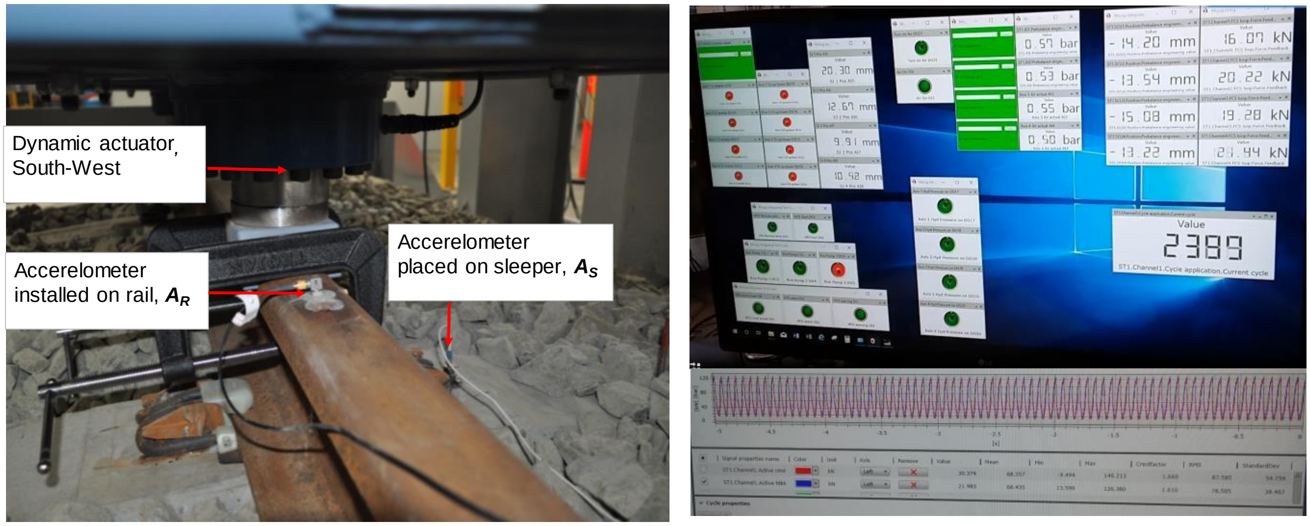

(a) (b)

Figure 6. (a) Installation of triaxial accelerometers on the rail and sleeper; (b) data acquisition system

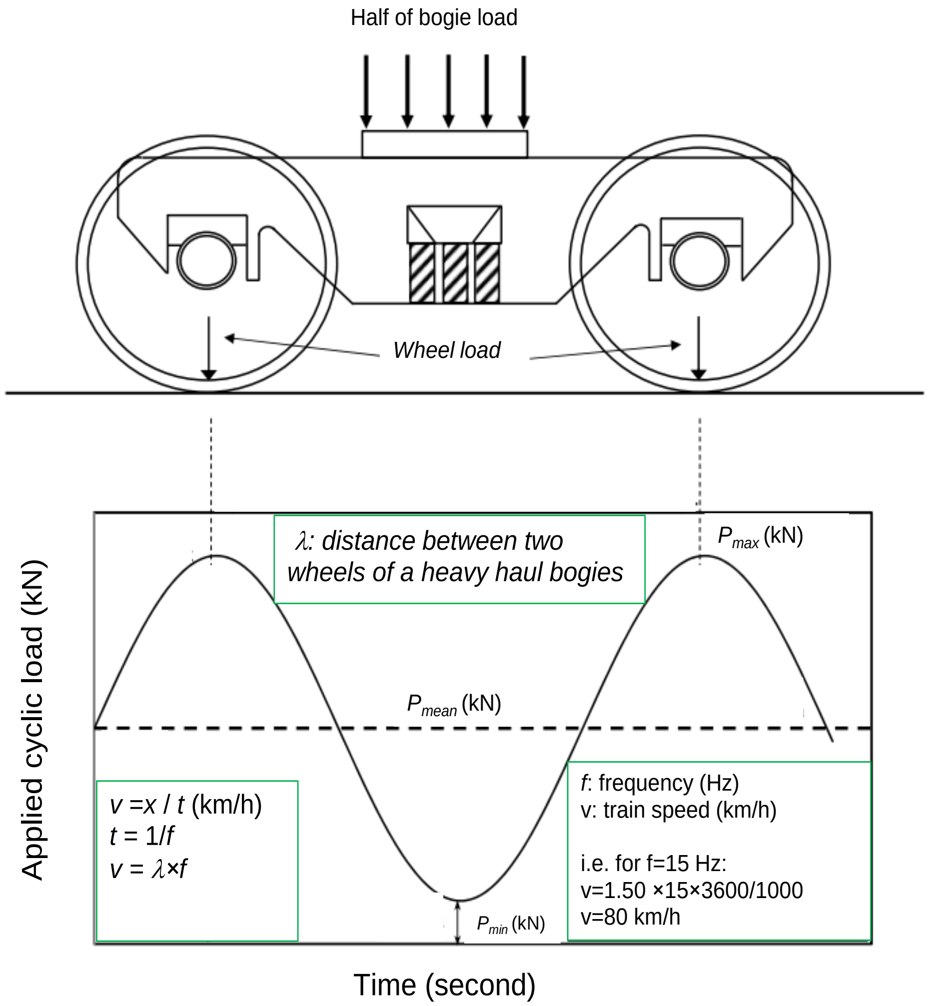

Figure 7. Typical schematic of axle load and applied cyclic load during the test

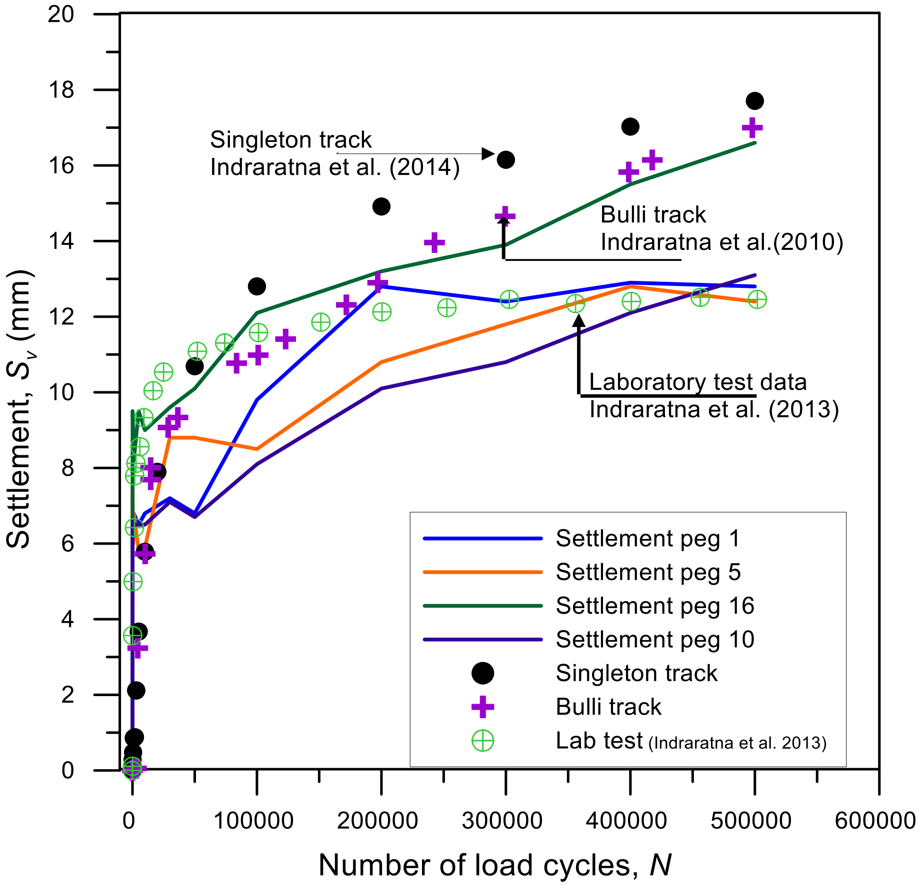

Figure 8. Measured settlements of the track at different locations in comparison with laboratory and field measurement data

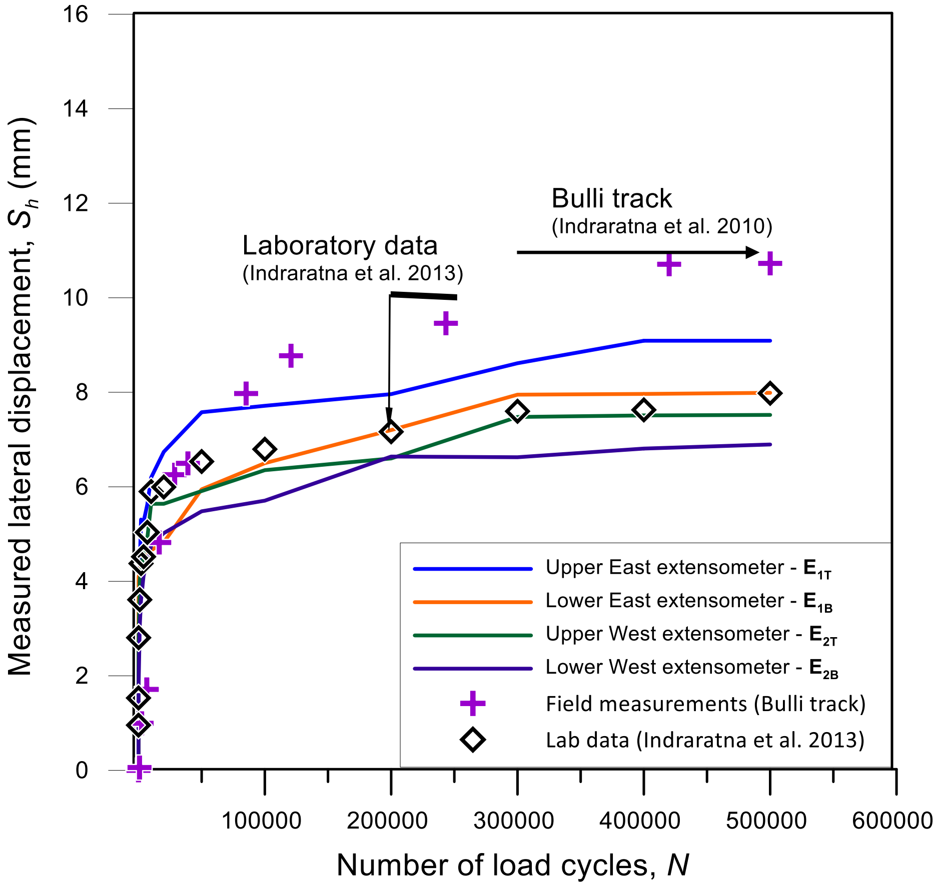

Figure 9. Measured lateral displacements at varying locations in comparison with laboratory and field measurement data

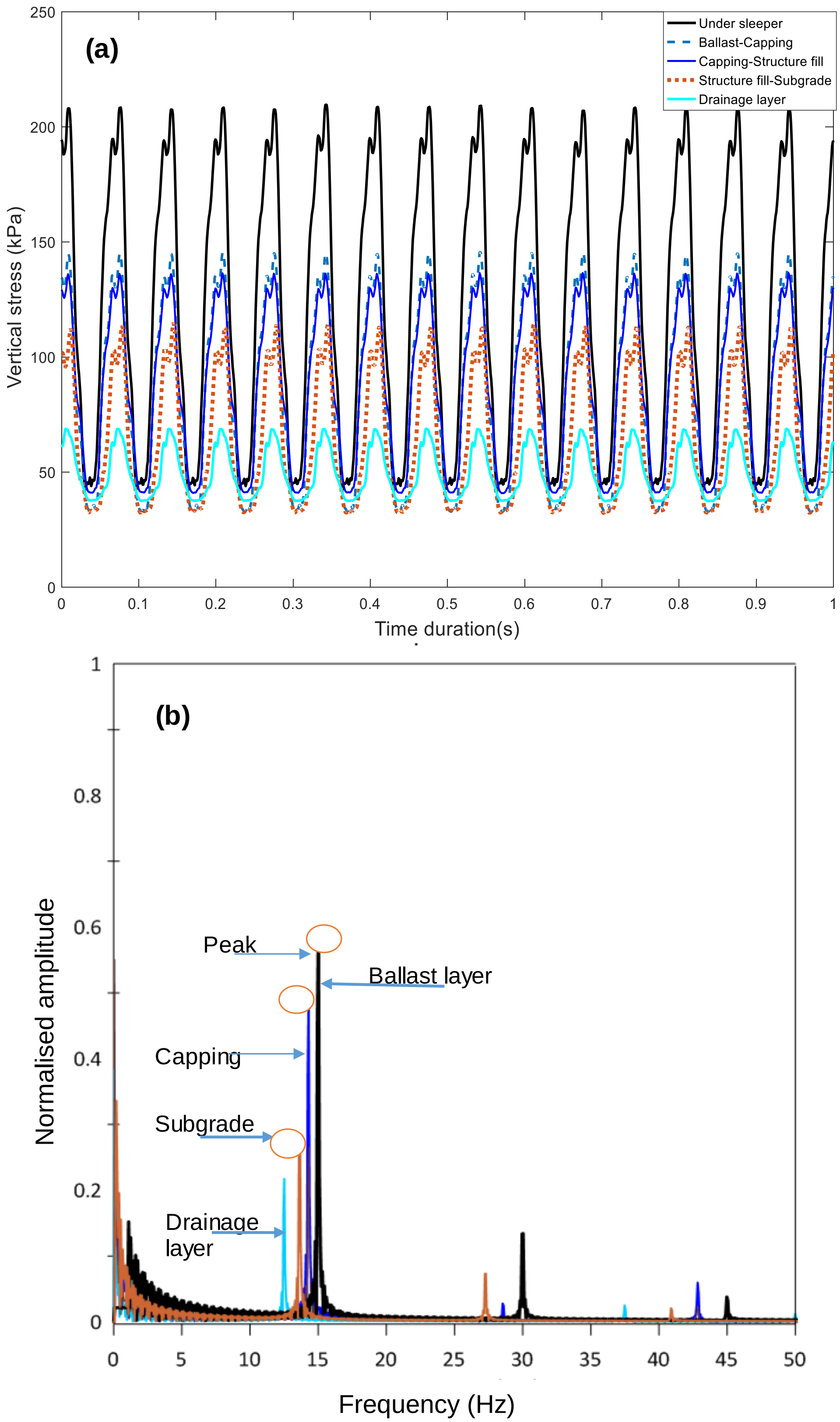

Figure 10. Typical cyclic vertical stress (σ_1) responses at varying depths measured by pressure plates: (a) time domain; (b) frequency domain

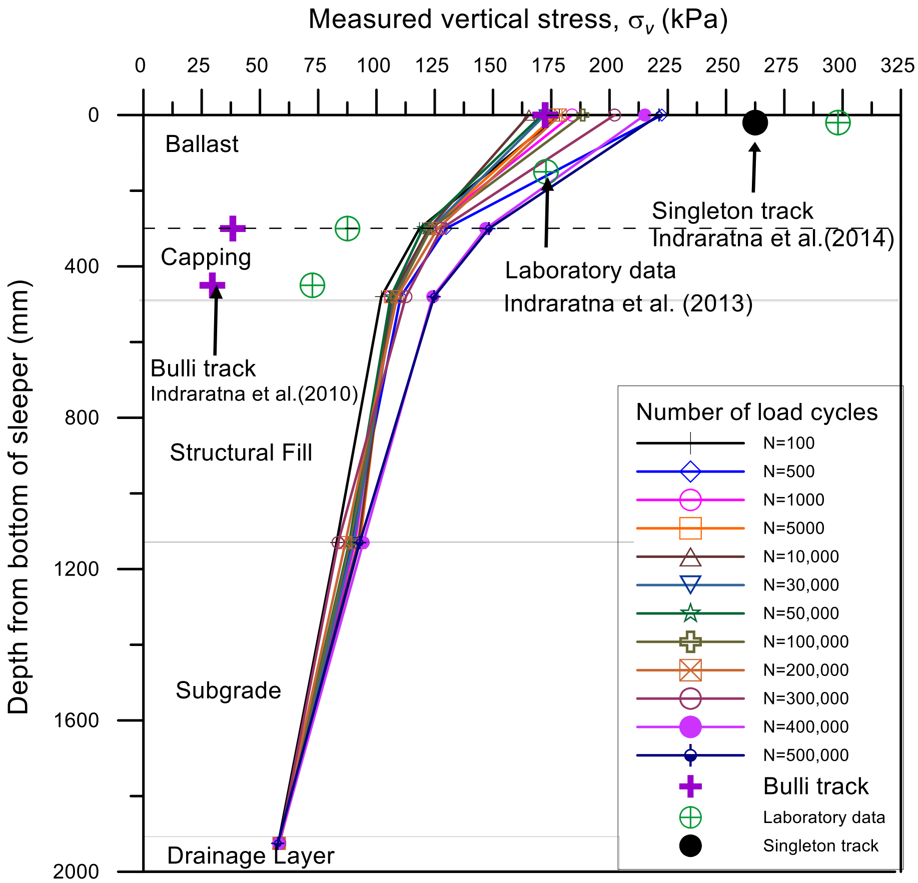

Figure 11. Variations of measured vertical stress (σ_v) with the depth of track substructure at varying load cycles (N)

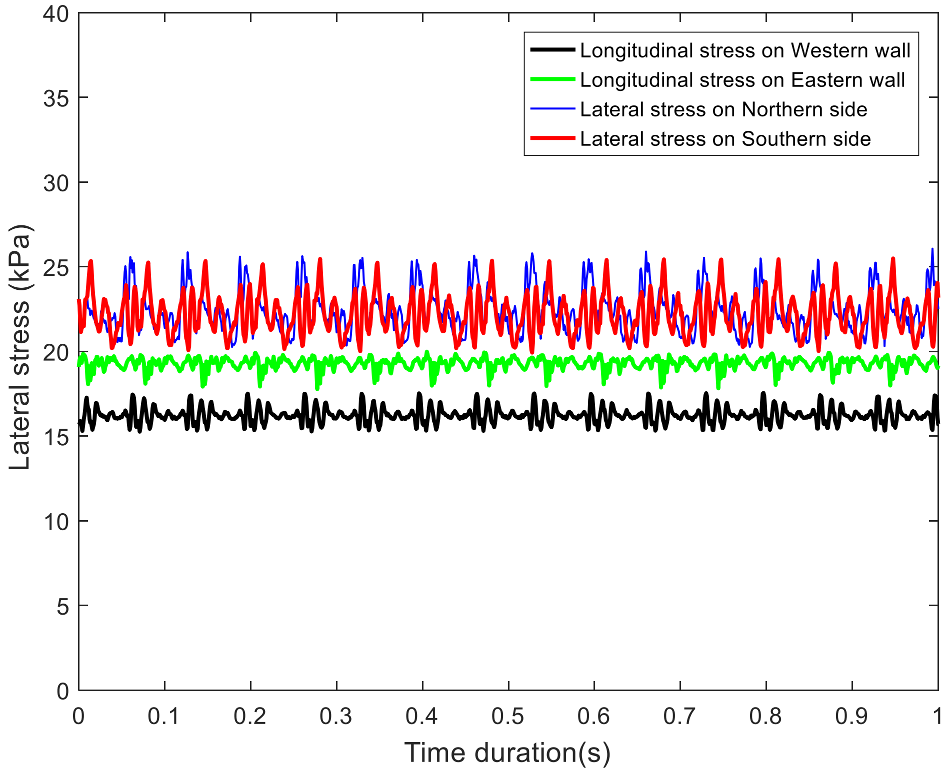

Figure 12. Typical responses of horizontal stresses (σ_2, σ_3) in ballast measured in longitudinal and transverse directions during the test

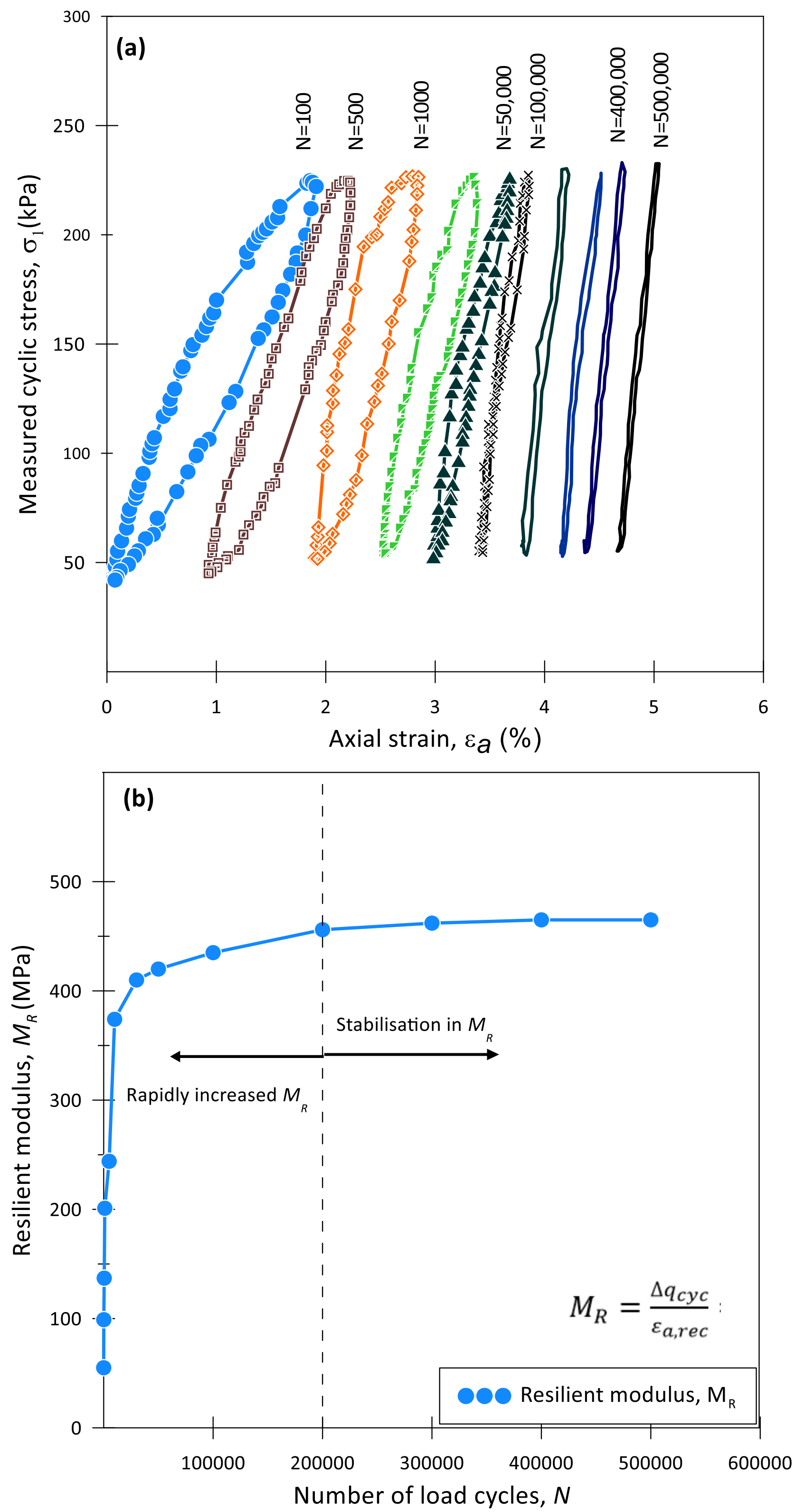

Figure 13. (a) Hysteresis cyclic stress– strain responses; and (b) measured resilient modulus (M_R)

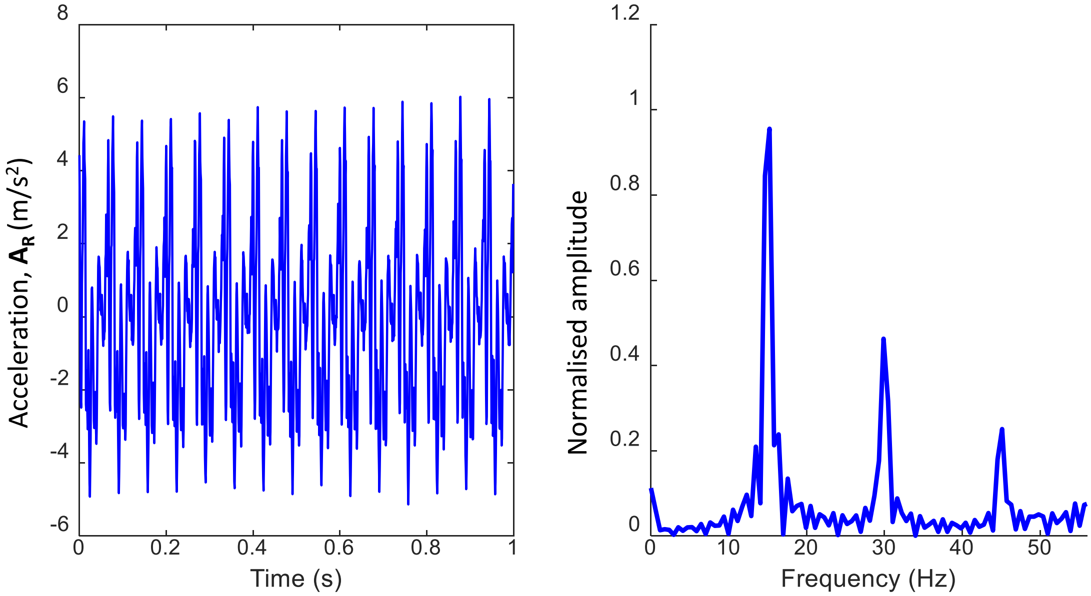

(a) Measured accelerations on rail

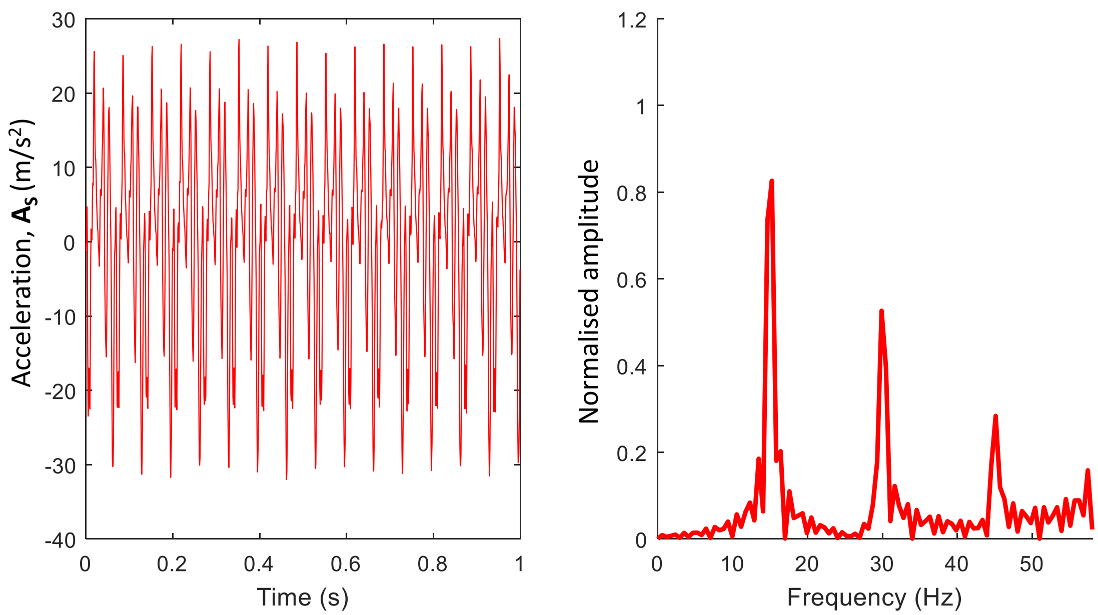

(b) Measured accelerations on sleeper

Figure 14. Measured accelerations of rail and sleeper during the test

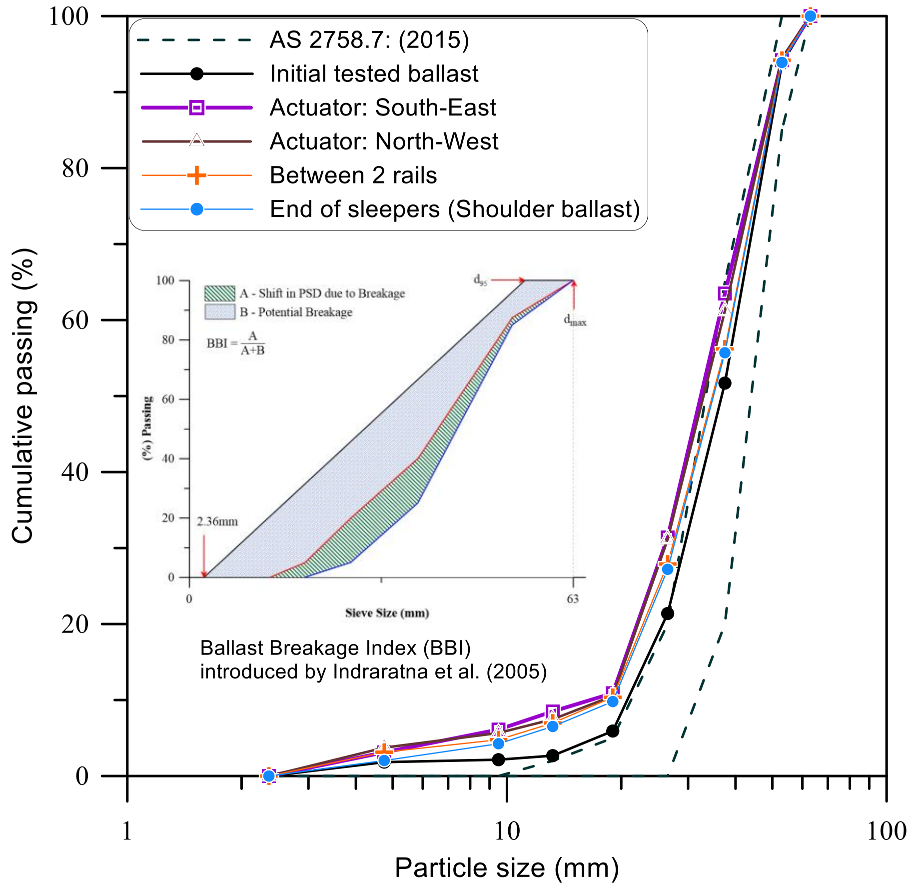

Figure 15. Measured changes in particle size distributions of ballast for quantifying ballast breakage index (*BBI*)

Large-scale Testing Facility for Heavy Haul Track

Buddhima Indraratna[1], Trung Ngo[2], Fernanda Bessa Ferreira[3], Cholachat Rujikiatkamjorn[4] and Ameyu Tucho[5]

[1]Distinguished Professor of Civil Engineering and Director, Transport Research Centre, University of Technology Sydney 15 Broadway, Ultimo, NSW 2007, Australia;
Founding Director, ARC Industrial Transformation Training Centre for Advanced Technologies in Rail Track Infrastructure (ITTC-Rail), University of Wollongong, NSW 2522, Australia.
Email: Buddhima.Indraratna@uts.edu.au

[2]Senior Lecturer, School of Civil and Environmental Engineering, University of Technology Sydney, 15 Broadway, Ultimo NSW 2007, Australia. Email: Trung.Ngo@uts.edu.au

[3]Postdoctoral Researcher, CONSTRUCT-Geo, Faculty of Engineering, University of Porto, 4200-465 Porto, Portugal. Email: fbf@fe.up.pt

[4]Professor, School of Civil and Environmental Engineering, University of Technology Sydney, 15 Broadway, Ultimo NSW 2007, Australia. Program Coordinator, ARC ITTC-Rail, University of Wollongong, NSW 2522, Australia. Email: Cholachat.Rujikiatkamjorn@uts.edu.au

[5]PhD student, School of Civil and Environmental Engineering, University of Technology Sydney, 15 Broadway, Ultimo NSW 2007, Australia. Email: AmeyuTemesgen.Tucho@student.uts.edu.au

Abstract: Given the substantially increased demand for increased axle loads of heavy haul trains, there is an imperative need to develop sustainable track infrastructure. When subjected to heavy axle loading, ballast aggregates rapidly break down, compromising the particle friction and associated load bearing capacity. Therefore, understanding the deformation and degradation (breakage) of ballast subjected to various boundary and loading conditions is crucial for improved track design and performance monitoring. Ideally, field testing should be carried out in real-life tracks to avoid laboratory scale and boundary effects, but field tests are often expensive, time-consuming and may disrupt rail traffic, hence not always feasible. A prototype test facility that can simulate appropriate axle loading and boundary conditions for standard gauge heavy haul tracks is presented in this paper. In collaboration with more than a dozen Universities and Industry organisations, Australia's first and only National Facility for Heavy-haul Railroad Testing (NFHRT) has recently been constructed and is now fully operational. This new facility enables a real-size (1:1 scale) instrumented track section to be subjected to continuous cyclic loading simulated via two pairs of dynamic actuators in synchronized operation. The results of a typical test are presented in this paper including the measured track settlement and lateral deformation, transient vertical and lateral stresses, rail and sleeper accelerations, resilient modulus and breakage of ballast. The test results show that an average track settlement of about 14 mm and lateral

displacements up to 9 mm are recorded after 500,000 load cycles. Subjected to a 25-tonne axle load, the maximum vertical stress measured at the sleeper-ballast interface is about 225 kPa and this attenuates with depth. The test results of this iconic facility are generally consistent with actual field measurements obtained in heavy-haul tracks located in the towns of Singleton and Bulli in the state of New South Wales, Australia.

Keywords: *Ballast, Rail geotechnics, Heavy hauls, Breakage, Prototype test*

1. Introduction

The current track infrastructure in various parts of Australia cannot sustain the increasing demand to transport freight to and from ports in regional and rural areas. This growth in demand for faster and heavier trains leads to an increase in the frequency and load intensity on track substructure. As a result, ballasted tracks settle differentially, particularly on weak subgrades with poor drainage, they become fouled due to clay pumping and ballast breakage, and the rail tracks buckle due to insufficient confining pressures from the shoulder ballast aggregates (Suiker and Borst 2003, Zhai *et al.* 2004, Indraratna *et al.* 2016, 2020a, Sayeed and Shahin 2017, Sol-Sánchez *et al*. 2020, Powrie *et al.* 2019, Guo *et al.* 2020).

Upon repeated train loading, fouling of tracks occurs along with ballast degradation. Fouling agents could decrease the shear strength of ballast and reduce the drainage capacity of ballasted track (Indraratna *et al*. 2011, Touqan *et al.* 2020). Huang *et al.* (2009) studied track problems associated with fouling issues in Wyoming, US and found that coal dust was the worst fouling agent for its impact on track substructure and roadbed. When the coal dust fouling percentage increased, the ballast shear strength steadily decreased. In particular, wet fouling was found to exacerbate this trend. Bian *et al*. (2017) investigated track problems related to the hanging of sleepers and showed that a hanging tie would lead to an increase in dynamic impact loading on the ballast and therefore further deteriorate the track substructure. Another track problem receiving increasing attention worldwide is associated with the transition zones between a ballasted track and a concrete bridge deck leading to enhanced dynamic load, differential settlement and accelerated track degradation (Hu *et al*. 2019, Mishra *et al*. 2014, Paixão *et al*. 2016).

Previous research carried out worldwide over the past decades has shown that ballast breaks down and progressively deteriorates under freight train loading. Over the years, heavy trains and faster passenger services have caused progressive deterioration of ballast which in turn results in loss of track geometry; this compromises safety and leads to more frequent maintenance (Selig and Waters 1994, Priest *et al.* 2010, Esveld 2014, Bian *et al.* 2020). In response, Australian railway companies are now emphasising on high-speed train corridors (5 routes across NSW) and heavier freight operations (Brisbane-Melbourne Inland rail) to achieve more efficient and cost effective services, particularly in the mining and agricultural sectors. One of the major challenges in delivering heavier and faster trains in Australia is not the immediate cost, but the geotechnical problems associated with poor ground conditions and soft coastal terrain (Budiono *et al.* 2004, Powrie *et al.* 2007, Sayeed and Shahin 2016, Indraratna and Ngo 2018).

The geotechnical challenges surrounding the performance of heavy hauls and high-speed trains on ballasted railway tracks are numerous, particularly when a track profile is built along the coastal areas of Australia (Indraratna *et al.* 2018a, Cai *et al.* 2020). Typical problems that arise in track substructure include: (i) ballast breakage; (ii) mud pumping in railway tracks constructed on clays and other soft soils (Indraratna *et al.* 2020b), consisting of the upward migration of subgrade clays and fine silts (slurry) under heavy traffic loading, which promotes settlement by "lubrication" and increases the risk of train derailment (Wang *et al.* 2020); (iii) ballast fouling due to voids in aggregates filled with relatively finer materials or fouling agents that reduce the shear strength and lead to poor drainage (Huang *et al.* 2009, Li *et al.* 2015, Touqan *et al.* 2020); and (iv) differential settlement and shear failure that may occur on tracks built on highly compressible soft clays residing in low lying terrain, and with very low undrained shear strength.

With this increasing demand for freight trains in Australia, it would be inappropriate to operate heavy hauls on ballasted tracks built on formation soils without testing on large-scale sections of prototype model track. Since existing Australian railway design practices are mainly based on static loading conditions, they are only suited to shorter trains with low axle loads travelling at speeds of less than 80 km/h. In some parts of Australia, freight trains can be almost 4 km long, so the ballast degradation (breakage), mud pumping of certain formation soils, and differential settlements must be studied and quantified to achieve a resilient track design and avoid hefty maintenance costs after construction (Raymond and Bathurst 1994, Brown *et al.* 2007, Biabani *et al.* 2016, Ferreira and Indraratna 2018, Indraratna *et al.* 2018b, 2019, Powrie *et al.* 2019).

Conventional triaxial testing is a popular approach of evaluating the strength and breakage of ballast aggregates in the laboratory (Raymond and Davies 1978, McDowell *et al.* 2005, Brown *et al.* 2007, Aursudkij *et al.* 2009, Sevi *et al.* 2009, Zhang *et al*. 2017, Harkness *et al.* 2016, among others). However, the discrepancy between the actual shape and size of particles in the field and the much smaller particle sizes adopted in conventional laboratory equipment contributes to inaccurate load and deformation responses measured in the laboratory. Moreover, since the bottom boundary is rigid and is typically less than 600mm deep, this boundary condition cannot simulate the actual field track substructure. This means that testing coarse aggregates in conventional apparatus can yield misleading results due to the disparity in size between particle and equipment and the limited depth of subgrade (Lim *et al.* 2005, Peijun and Xubin 2007, Indraratna *et al.* 2018a). Previous large-scale triaxial tests carried out by many researchers have shown that the ratio between the size of the testing chamber and the particle size must be greater than 7-8 to reduce boundary effects (Marachi *et al.* 1972, Marsal 1973, Lade *et al.* 1996).

To alleviate these size dependent issues, examine a range of Australian ground conditions and integrated track components, the National Facility for Heavy-haul Railroad Testing (NFHRT) was the first to be designed and built in-house at Russell Vale, NSW, Australia. The NFHRT allows for a full size instrumented railway track section to be tested so that the effects of track substructure can be captured. Such a facility could not be established through purely commercial means; rather, it was designed and built in close cooperation with the Australian rail industry, a consortium of transport research centres in several Australian Universities and the Australian Research Council, c/o Ministry of Education, under the leadership of the first author.

In fact, the Australian rail industry has strongly promoted the state-of-the-art test facilities for heavy haul track modelling, and this was the main driver for constructing the first NFHRT under Commonwealth government funding channelled through the Australian Research Council. In particular, the NFHRT was designed and built in close cooperation with Australian Rail Track Corporation (ARTC) and Sydney Trains, whereby an array of typical ground conditions and integrated track components were considered in relation to the national flagship project Melbourne to Brisbane Inland Rail (MBIR), one of the longest heavy haul tracks to be completed soon.

Although similar test facilities have also been built in other countries (Brown *et al.* 2007, Bian *et al.* 2014, Abadi *et al.* 2016, Li *et al.* 2018, Bian *et al.* 2020, Hasnayn *et al.* 2020), these were built mainly for high-speed passenger trains capturing more favourable foundation characteristics in cold regions (e.g., stiff boulder clays and glacial tills) or for concrete slab tracks used for short high speed commuter trains (Zhang *et al.* 2019a, 2019b, Zhai *et al.* 2020, Li *et al.* 2020). Conversely, the Australian soft soil terrains for very long heavy axle freight trains are considerably different, including highly compressible black soils and deposits of upper Holocene soft clays. In this regard, the overall objective of the NFHRT is to contribute to innovative and more cost-effective designs for heavy haul tracks built on an array of problematic ground conditions.

It is noteworthy that the true moving load effect cannot be properly modelled using the NFHRT, as the cyclic loading is applied by four dynamic actuators in synchronized operation. This facility is mainly for simulating heavy haul ballast tracks for high axle freight trains that operate at low speeds. At high speeds exceeding say 130 km/h, there is significant principal stress rotation under moving loads, which cannot be simulated accurately by this facility as it only has two pairs of actuators. For simulating a true moving load at high speeds (exceeding say 130 km/h), one needs more than two pairs of actuators acting along a greater number of sleepers (Bian *et al.* 2014). In addition, the dynamic and impact effects due to track irregularities could not be captured in these model tests, and this is a limitation of the current study.

The main objective of this research is to introduce Australia's NFHRT that has recently been constructed and is now fully operational, as well as to validate the observed results against past field measurements available from heavy haul tracks located in the towns of Bulli and Singleton (NSW, Australia). The results of the first test are presented in this paper and compared with the available field monitoring data. These results will also serve as a benchmark for future tests considering varying track substructure conditions (e.g., excessive settlement of compressible soft soils and instability of saturated subgrade including mud-pumping), the effectiveness of artificial inclusions such as geosynthetics for improved track stability and the vibration mitigation of carriage-track-foundation interactions using damping elements made of recycled rubber. Details of the NFHRT, test set up, instrumentation, and the results of the first test are presented in the following sections.

2. National Facility for Heavy-haul Railroad Testing

2.1. Design and construction of the NFHRT

The NFHRT consists of a large-scale laboratory test facility that allows the testing of a fully instrumented ballasted track section at 1:1 prototype scale. It includes a test pit, loading frames, a hydraulic servo-controlled system with four dynamic actuators and a high capacity hydraulic power unit, an electrical system, an instrumentation and data acquisition system, and a 5-tonne overhead crane. A schematic of the NFHRT is shown in Figure 1a.

A 6.0m-long × 6.0m-wide × 2.3m-deep test pit was excavated, and four 900mm-thick reinforced concrete walls and a 600mm-thick reinforced concrete floor were then constructed (Fig. 1b). The hydraulic actuators and power unit of the NFHRT were designed, fabricated and then assembled (Fig. 1c). A trench for the hydraulic pipework (9.13m long × 1.35m wide × 0.5m high) was built with reinforced concrete walls (Fig. 1d).

Track materials such as ballast, capping, structural fills, subgrade, and a drainage layer are installed beneath a rail-sleeper assembly to accurately estimate their actual response when subjected to realistic loading conditions. A hybrid hydro-electrical substation with heavy duty hose connections from the hydraulic pipework to the four dynamic actuators provide the cyclic loading capable of simulating up to 40-tonne axle trains operating at speeds up to 200km/h. The actuators apply the designed cyclic loading directly onto the rails and are fully controlled through the computerised operating system also linked to an automated data acquisition system.

2.2. Materials and test procedures

In this first test, a 75mm thick drainage layer consisting of coarse grained gravel was placed at the bottom of the test pit (Fig. 2a) overlain by a geotextile filter to avoid clogging. A 795mm-thick layer of fine-grained subgrade soil (classified as CL according to the Unified Soil Classification System) was then installed and spread by a mini excavator. The subgrade was compacted in four sub-layers to a dry unit weight of 16.5 kN/m^3 (moisture content, w=20%) using a lightweight compaction plate. Pressure cells, soil moisture sensors and pore water pressure gauges were installed within the subgrade to measure the respective parameters during testing (Fig. 2b and 2d). An irrigation system consisting of a series of perforated pipes wrapped with a geotextile filter was installed in the subgrade layer to control the water content and the degree of saturation of the track foundation (Fig. 2c).

A 650mm-thick structural fill layer (moisture content, w=11.5%) was placed on top of the subgrade and compacted in sub-layers of 150 mm thick to achieve a dry unit weight of 18.5 kN/m^3, using similar procedures to those described earlier for the subgrade layer. A 180mm thick capping layer (sub-ballast) consisting of a sand and gravel mixture was then placed over the structural fill (Fig. 3a) and compacted in two sub-layers (90mm thick) to a dry unit weight of 19.5 kN/m^3, corresponding to about 90% of γ_{dmax} based on the standard Proctor compaction method in accordance with AS 1289.5.1.1 (2017). A heavier compaction plate was used to compact the sub-ballast material, giving the higher compaction requirements of this layer. To ensure all the materials from the bottom subgrade layer to the capping layer had been compacted to the desired unit weight, sand cone tests were conducted following the ASTM D1556 (2007) (Fig. 3b). Pressure cells and horizontal displacement transducers were then placed over the capping layer, as shown in Figure 3c.

Ballast (latite basalt aggregates) was obtained from the Bombo quarry, about 100km South of Sydney, then cleaned and sieved following the Australian Standards (AS 2758.7, 2015). The ballast was compacted in three sub-layers (100mm-thick) to achieve a density of nearly 16 kN/m^3 and the total thickness of the load-bearing ballast was 300mm, as typically used in actual Australian heavy-haul tracks (Fig. 3d). The selected densities for the track substructure layers are comparable with other studies reported earlier by Suiker *et al.* (2005), Aursudkij *et al.* (2009), Biabani *et al.* (2016) and Anderson and Fair (2008).

A system of rails and sleepers provided by the Australian Rail Track Corporation (ARTC) was laid onto the ballast layer (Fig. 3e) and additional ballast aggregates were then placed to simulate the crib and shoulder ballast. The loading frames were bolted in position and the four dynamic actuators were installed to apply a dynamic train loading (Fig. 3f). The particle size distribution (PSD) of the ballast, capping, structural fill and subgrade materials used for this test are shown in Figure 4.

2.3 Instrumentations

Figure 5a presents a plan view of the instrumentation installed into the track substructure such as settlement pegs (1-16), horizontal displacement transducers (E_{1T}, E_{1B}, E_{2T} and E_{2B}), pressure cells and the positions of the rail and sleeper system. Figure 5b is a cross section (North-South section) of the testing pit showing the locations of the sensors. Twenty rapid response hydraulic pressure cells were installed at different locations and depths to measure the transient vertical and horizontal stresses; sixteen settlement pegs were installed at varying depths in the structural fill, capping and ballast layers to measure the permanent vertical deformations. Four horizontal displacement transducers were placed bellow the loaded sleepers at two different depths (i.e., two of which were installed underneath the sleepers and the other two were installed at the bottom of the ballast layer). Two triaxial accelerometers were installed on the rail and sleeper to measure acceleration (vibration) during the tests (Fig. 6a). In addition, eight pore water pressure transducers, four moisture sensors and four water potential sensors were placed in the subgrade to monitor the excess pore pressure and/or the changes of water content and water potential, depending on the moisture conditions of the subgrade layer in each test. These sensors were installed in the subgrade layer for future tests considering the submergence of subgrade through the irrigation system to study track problems associated with flooded track conditions in low-lying coastal areas as well as the saturated subgrade instability, e.g., mud-pumping. Measurements from these sensors will be available for the future tests when the track substructure is made to be saturated.

All the sensors and instruments were calibrated before testing. A data acquisition system controlled by a host computer automatically recorded all the data collected during the test (Fig. 6b). The selected sample rate (data logging frequency) for all the signals was 1200 Hz.

2.4 Cyclic loading characteristics

In this test, the load was selected based on a typical Australian freight train having an equivalent 25-tonne axle load. Therefore, a maximum load of 12.5 tonnes (125 kN) was applied by each dynamic actuator, simulating a realistic wheel load. The applied loading characteristics are schematically shown in Figure 7 corresponding to a vertical load of P_{max}=125 kN, P_{min}=15 kN and P_{mean}=70 kN, corroborating to a freight train of 25-tonne axle load. The minimum load of 15kN ensured continual contact between the dynamic actuators and the rails during the test.

The applied frequency of f=15 Hz in the experimental program is assumed to cover a realistic range of heavy haul train speeds of 60-80km/h on standard gauge tracks, based on Indraratna et al. (2011), Sun et al. (2016) and Navaratnarajah et al. (2018). In reality, the frequency is not only dependent on the train speed but also on track geometry, bogey spacing, rest periods, variations in cyclic and impact loading among other variables~~The cyclic load was applied at a frequency of *f*=15 Hz that simulated an operational speed of less than 80 km/h, mimicking the upper bound of heavy haul trains in Australia~~. For typical Australian freight train~~ speeds (50-60 km/h in most cases, with a maximum of 80km/h for very long straight sections)~~, the loading frequency was estimated by considering the distance between the last wheel of the front bogie and the first wheel of the next bogie on a standard gauge track in Australia. As the axle distance is much smaller than the length between bogie centers (L_b) or vehicle length, the two rear axles of a leading wagon and two front axles of a trailing wagon would represent the highest generated frequency (Indraratna *et al*. 2011). Heavy haul trains in Australia are often 4-5 km long and they travel on standard gauge tracks at relatively low speed (@ 40-60 km/h in most cases and rarely exceed 70k/h), and the applied frequency in the laboratory is indeed corroborated with the track geometry and train speed (e.g. Indraratna et al. 2011, Sun et al. 2016, Navaratnarajah et al. 2018). It is also noticed that there can be several variables including the sleeper spacing, speed of train, track irregularities, occasional impact loading, influence of rest periods, variation in cyclic loading due to non-uniform axle spacing etc. that can contribute to the real-life frequency in contrast to the simplified (constant) experimental magnitude of frequency.

The actuators worked in synchronised pattern up to N=500,000 load cycles to simulate the realistic repeated loading on the rails, but given the limitation of having only two pairs of actuators, the ideal simulation of moving loads from the bogies of a long train was not possible. As mentioned earlier, the design of this equipment is reasonable for slow moving heavy haul trains in Australia, but not for representing high speed passenger trains where significant principal stress rotation occurs under fast moving loads. In addition, it is noted that the loading sequence capturing rest periods is not considered in this study. This is because the worst conditions occur when very long heavy haul trains apply continual loading over a substantial period of time, and busy freight tracks in the mining hubs have relatively small rest periods. For example in Western Australia different mineral ore trains can travel over very long distances at slow speeds (40-60 km/h) from source to port (sometimes up to 300 km) regularly most of the day, and the ballast relaxation during relatively short rest periods between these slow-moving trains can be ignored. For instance for iron ore trains that can be up to 6 km long moving at only 40 km/h, the worst-case scenario simulated in the laboratory is without any rest period, so that the fatigue of ballast is maximised during testing to determine the maximum deformation, i.e. settlement and lateral movement. Both the axle load and loading frequency influence the resulting settlement, but the axle load magnitude is more dominant than the frequency. Nevertheless, the load frequency must still be highlighted, because that is the only loading parameter in cyclic laboratory testing that is related to the train speed (Esveld, 2014; Indraratna et al. 2011). In other words, the number of axle loads passing through a specific in situ reference point (worksite) over a given period of time is related to the frequency.

3. Results and discussion

3.1. Measured vertical settlement

Figure 8 shows the accumulated track settlement after being subjected to a 25-tonne axle load at a frequency of f=15 Hz, as recorded by the settlement pegs installed below the sleepers (S_1, S_5, S_{10} and S_{16} – Fig. 5a). It can be concluded that the vertical displacement (S_v) of ballast increased rapidly up to about N=50,000 cycles due to its initial densification and subsequent packing as the corners of the sharp angular ballast aggregates began to break (S_v = 6.2 mm to 8.7 mm). However, once the aggregates began to stabilise the rate of vertical displacement gradually decreased and remained relatively constant after N=200,000 cycles (S_v = 8.7 mm to 12.1 mm). This shows the aggregate density has reached threshold compression and would resist further rearrangement and densification with additional cycles. The measured final track settlement, taking the average of the four settlement pegs, was about S_v=14.2 mm. These observations are in agreement with the data obtained in the laboratory (Indraratna *et al.* 2013) and the field measurements taken at the Bulli and Singleton tracks (Indraratna *et al.* 2010, 2014). It is noted that while the track settlement measured at the Bulli track matched those measured at the NFHRT facility, field data from the Singleton track showed higher vertical settlement, especially after N=200,000 cycles. This could be due to the track section at Singleton being built on a flood plain with a 7-10 m thick layer of alluvial silty clay, which could lead to greater vertical deformation of the track.

3.2. Measured lateral displacement

Figure 9 presents the lateral displacement (S_h) of the ballast layer as recorded by the four horizontal displacement transducers, two of which (E_{1T}, E_{2T}) were placed underneath the sleepers and the other two (E_{1B}, E_{2B}) were installed at the boundary between the ballast and capping layers at the bottom of the ballast layer (Fig. 5). The lateral displacement of ballast measured at the Bulli track and from laboratory tests performed earlier (Indraratna *et al.* 2010, 2013) are also shown in Figure 9 for comparison purposes. The measurements from all the displacement transducers show consistent increases in lateral displacement with increased N. The ballast aggregates showed a significant horizontal spread (S_h=5.8 mm - 6.2 mm) within the initial N=100,000 cycles, followed by a gradual increase in S_h up to N=300,000 cycles, after which S_h remained nearly constant towards the end of the test. The final horizontal displacement of the track varied from S_h=6.8 mm - 9.1mm, depending on the location of each measurement. This trend is similar to those observed earlier in actual rail tracks and in the laboratory by Indraratna *et al.* (2013). However, the data from the field trial at Bulli track show higher lateral displacements than those measured at the NFHRT. This is possibly because moving freight trains generate greater impact forces due to wheel or rail irregularities such as flat wheels, dipped rails, expansion gaps and rail corrugations, which could accelerate the degradation and lateral spreading of ballast (Auersch 2015, Ferreira and Indraratna 2018, Indraratna *et al*. 2020a). Furthermore, in the NFHRT two aluminium panels (200mm-high) were placed on both sides of the shoulder ballast to maintain track geometry during the commissioning process, which may have provided some additional confinement to the ballast layer leading to slightly lower lateral deformations when compared to the field measurements at Bulli track.

3.3. The vertical and lateral stresses

Figure 10a shows the typical vertical stresses recorded over time at different depths of the track substructure (from the top surface of the ballast to the drainage layer) during the test. Pressure cells were placed between the sleepers and ballast, beneath the ballast layer, between the capping and structural fill, and on top of the subgrade and drainage layers to measure the stresses at different depths (Fig. 5b). Under a 25-tonne axle load the maximum vertical stress at the sleeper-ballast interface is about $\sigma_v = 225$ kPa, and the σ_v attenuates with depth. The maximum vertical stresses at the top surface of the capping layer, the structural fill, the subgrade and drainage layers are measured as $\sigma_v = 151$, 132, 98, and 54 kPa, respectively. The vertical stresses at different depths plotted on the frequency domain are shown in Figure 10b. Here, the cyclic response of the stresses recorded in the ballast layer peaks at f=15Hz, but these peaks decrease slightly in the underlying layers showing how the loading frequency attenuates with depth.

Figure 11 illustrates the vertical stress (σ_v) measured at different layers of the track substructure and its variation with the number of load cycles. It is evident that the dynamically induced stress in the ballast layer increases with N (e.g., at the first N=500 cycles, σ_v =175 kPa, and then σ_v continues to increase to σ_v =225 kPa at the end of the test, N=500,000 cycles). On the other hand, the vertical stress σ_v decreases with the depth of the test pit where the σ_v recorded in the subgrade and drainage layers is approximately 95 kPa and 48 kPa, respectively. The vertical stresses obtained in a previous laboratory study and on the field tracks (Singleton and Bulli tracks) are also plotted in Figure 11 for comparison purposes (Indraratna *et al.* 2010, 2014, Navaratnarajah *et al.* 2018). Given that the laboratory equipment used in the previous study has a limited boundary, only the stresses up to a depth of 500 mm below the surface of ballast are presented. The σ_v reported in previous studies shows some fluctuations where σ_v between the sleeper and ballast varies from 172 kPa to 300 kPa, and then decreases to about 38 kPa (Bulli track) and 87 kPa (laboratory test) when measured at the top surface of the capping layer.

Figure 12 shows the horizontal stresses (σ_h) in the ballast layer obtained in the longitudinal direction parallel to the rails and in the transverse direction parallel to the sleepers. Data were monitored by two pressure cells placed at the northern and southern sides of the track (lateral confinement in the transverse direction - σ_3) and two pressure cells placed on the eastern and western walls to measure the longitudinal stresses (σ_2). It is seen that the horizontal stress (σ_h) remains almost unchanged during the test. Lateral confinement in the transverse direction, commonly known as the confining pressure (σ_3), is around σ_3=22 kPa to 25 kPa during the test, whereas the longitudinal stress (the intermediate stress, σ_2) varies from σ_2=15 kPa to 20 kPa. The lateral stresses in the transverse direction exceeded those in the longitudinal direction possibly because the latter were measured by pressure cells fixed to the vertical steel walls, which were further away from the locations of load application (actuators). The confining pressures measured in this study are generally consistent with those recorded during previous field monitoring programmes carried out in Australian heavy-haul tracks.

3.4. Measured resilient modulus

The resilient modulus (M_R) of ballast can be calculated as the ratio between the deviatoric stress (Δ_{qcyc}) and the resilient (recoverable) axial strain ($\varepsilon_{a,rec}$) during loading-unloading stage, as given by:

$$M_R = \frac{\Delta q_{cyc}}{\varepsilon_{a,rec}} = \frac{q_{cyc,max} - q_{cyc,min}}{\varepsilon_{a,rec}} \qquad (1)$$

The resilient (recoverable) axial strain ($\varepsilon_{a,rec}$) was obtained at a given number of loading–unloading cycles (N) using the data bursting approach to determine the resilient modulus (M_R) of ballast. During the test, the relevant sets of data bursting were initiated at N= 1, 50, 100, 500, 1000, 5000, 10,000, 50,000, 100,000, 200,000, 300,000, 400,000, and 500,000; and the recoverable axial strains ($\varepsilon_{a,rec}$) during unloading were determined by subtracting the measured axial strains of the corresponding loading-unloading cycle. Figure 13a shows the typical stress-strain hysteresis loops plotted for a given load cycle. It can be observed that the areas of the hysteresis loops are reduced as the number of load cycles (N) increases, which indicates that ballast aggregates become more compacted and respond more elastically with increased N. The variation of resilient modulus M_R with N presented in Figure 13b shows a rapid increase of M_R within the first N = 200,000 cycles (M_R=462 MPa), after which the rate at which M_R increased becomes marginal. The rapid compression and densification of ballast during the initial load cycles increases track stiffness, leading to a rapid increase in M_R at the beginning of the test. After N=200,000 loading cycles the ballast aggregates may move to the shakedown stage, which causes the M_r to remain relatively unchanged (Le Pen *et al.* 2016, Sun *et al.* 2019).

3.5. Rail and sleeper acceleration

As mentioned, two triaxial accelerometers (A_R and A_S) were installed on the rail and sleeper to measure acceleration (vibration) during the tests. The acceleration of the rail and sleeper plotted in time and frequency domains are shown in Figure 14. Here, the accelerations measured at the sleeper (A_S) are greater than those recorded at the rail (A_R), with a maximum value of A_s = 27.2 m/s^2 compared to the highest value of A_R = 5.6 m/s^2. It is noteworthy that the rails were connected to six concrete sleepers creating a stronger system that could prevent from excessive vertical vibration, while the edge of sleeper was more prone to vertical displacement due to sitting on the discrete ballast aggregates. The accelerations were measured at the end of the test where the ballast shoulder has significantly displaced laterally and could cause the condition of hanging sleeper. As a result, there was a reduction in lateral confinement applied to the sleepers that resulted in increased sleeper displacement and associated acceleration.

The acceleration (vibration) in the time domain is converted into the frequency domain by the fast Fourier transform (FFT), as shown in Figure 14. It is observed that the responses reach their maximum peak values at an approximate frequency of f_1 = 15 Hz, while some smaller peaks are reached at higher frequencies (Kouroussis *et al.* 2009). The f_1 frequency is identical to the cyclic loading applied by the dynamic actuators, which indicates that the response of the track substructure to acceleration is in the same phase as the applied loading frequency.

3.6. Measured ballast breakage

After the test, ballast aggregates at four different locations (underneath two actuators, between the two rails, and at the shoulder ballast) were recovered separately for quantifying ballast breakage. This ballast was then passed through standard sieves to obtain the particle size distribution (PSD), as shown in Figure 15. Indraratna *et al*. (2005) introduced a new method to quantify ballast degradation under cyclic loading, which leads the PSD curve of ballast to shift towards the smaller size particles due to breakage. By recognising this shift as the degradation indicator, the ballast breakage index (*BBI*) can be calculated using Equation 2

$$BBI = \frac{A}{A+B} \quad (2)$$

where, A is the shift in PSD due to ballast breakage under cyclic loading, and B is the potential breakage or the area between the arbitrary boundary of maximum breakage and the final particle size distribution. It is noted the upper and lower limits of BBI are 0 (no breakage) and 1, respectively. A summary of the sieve analysis performed before and after the test for quantifying ballast breakage (BBI) is presented in Table 1. Measured breakage denotes that ballast aggregates collected directly underneath the actuators had the highest amount of breakage, estimated as $BBI_{1,2}$ = 0.143 and 0.115, whereas the ballast collected from between two rails (crib ballast) and the edge of a sleeper (shoulder ballast) have $BBI_{3,4}$ = 0.085 and 0.075, respectively. The ballast underneath the actuators experiences more breakage because these aggregates carry the cyclic loads directly from the dynamic actuators and also deal with the vibration transferred from the sleepers. As a consequence, these aggregates are more prone to breakage. The results also show that the average BBI for ballast samples collected underneath the actuators (BBI = 0.129) was slightly higher than that obtained for ballast aggregates recovered from beneath the sleeper and rail seat in the actual heavy-haul track at Singleton after the same number of load cycles (Nimbalkar and Indraratna 2016). In fact, in the NFHRT the load is continually applied over the same sleepers for 500,000 cycles, which results in a slightly higher amount of ballast crushing when compared to actual field measurements.

4. Conclusions

This paper described the construction and testing process of the new Australia's National Facility for Heavy-haul Railroad Testing (NFHRT), a prototype test facility that allowed investigating the performance of a real-size instrumented track section when subjected to continuous cyclic loading applied via two pairs of dynamic actuators. The first test was carried out under a 25-tonne axle load applied at a frequency of 15 Hz to cover a realistic range of heavy haul train speeds of 60-80km/h on standard gauge tracks~~simulate a freight train travelling at a speed of approximately 80 km/h~~. The results from this first test, including the measured track settlement and lateral deformation, transient vertical and lateral stresses, rail and sleeper accelerations, resilient modulus and breakage of ballast were presented and compared with actual field measurements obtained in heavy-haul tracks located in the towns of Bulli and Singleton (New South Wales, Australia).

The obtained results were generally consistent with real-life measurements undertaken during the aforementioned field monitoring programmes. An average track settlement of about 14 mm and lateral deformations up to 9 mm were recorded after 500,000 load cycles. Any small discrepancies between the test results and the actual field measurements may be associated with boundary conditions and loading simulations. For instance, the lateral deformation of the ballast layer recorded in the field trial conducted at Bulli exceeded that measured in the NFHRT. This is partially because moving freight trains generate greater impact forces due to wheel or rail irregularities, which could accelerate the lateral spreading of ballast. On the other hand, the breakage of the load-bearing ballast estimated at the end of the test ($BBI = 0.129$) was found to be slightly higher than that measured in the actual rail track at Singleton, which can be related to the fact that in the NFHRT the load was continually applied over the same sleepers for 500,000 cycles, thus resulting in a higher extent of ballast degradation.

It is noteworthy that the true moving load effect was not properly modelled in the test reported herein, as the cyclic loading was applied by four dynamic actuators in synchronized operation. In spite of this limitation, the obtained results for these relatively low speeds (≈ 80 km/h) were acceptable as the facility mimicked the cyclic loading appropriately. However, at very high speeds the results may deviate from accuracy when fast moving loads must be simulated correctly with more than two pairs of actuators acting along a greater number of sleepers (Bian *et al*. 2014).

When compared to smaller-scale or conventional laboratory test facilities, the NFHRT enabled to mitigate boundary effects and more realistically simulate Australian track conditions (often involving problematic subsoils) in a controlled laboratory environment. The test reported in this paper was aimed at simulating the conditions prevailing in typical Australian heavy-haul tracks. Additional tests will be carried out in the future to examine the benefits of artificial inclusions, such as geosynthetics and recycled rubber products, as well as the influence of different substructure materials (including recycled waste materials) on track performance, which will facilitate innovative and more sustainable designs for enhanced stability and resiliency of heavy haul tracks.

Acknowledgements

This study was carried out by the ARC Industrial Transformation Training Centre for Advanced Technologies in Rail Track Infrastructure (ITTC-Rail) and was funded by the Australian Government

(IC170100006). The financial support from the Australian Research Council through the Linkage Infrastructure, Equipment and Facilities scheme (LE140100010) is gratefully acknowledged. The authors also appreciate the insightful collaboration and assistance of Australian Rail Track Corporation (ARTC), Sydney Trains, Australasian Centre for Rail Innovation (ACRI), SMEC, RM CRC, among others, for their continuous cooperation and support. The authors are also grateful to UOW's technical staff, namely, Mr Alan Grant, Mr Duncan Best, Mr Cameron Neilson, and Mr Ritchie McLean for their assistance during the construction and commissioning of the NFHRT.

References

Abadi, T., L. Le Pen, A. Zervos and W. Powrie (2016). A Review and Evaluation of Ballast Settlement Models using Results from the Southampton Railway Testing Facility (SRTF). Procedia Engineering 143: 999-1006.

AS 2758.7 (2015). Aggregates and rock for engineering purposes, Part 7. Railway Ballast. Standards Australia, NSW, Australia.

AS 1289.5.1.1 (2017). Methods of testing soils for engineering purposes, Method 5.1.1: Soil compaction and density tests - Determination of the dry density/moisture content relation of a soil using standard compactive effort. Standards Australia, NSW, Australia.

ASTM D1556 (2007). Standard test method for density and unit weight of soil in place by the sand-cone method. ASTM International, West Conshohocken, PA, USA.

Anderson, W.F., and Fair, P. (2008). Behavior of railroad ballast under monotonic and cyclic loading. Journal of Geotechnical and Geoenvironmental Engineering 143(3): 316–327.

Auersch, L. (2015). Force and ground vibration reduction of railway tracks with elastic elements. *Journal of Vibration and Control,* **21**(11), 2246-2258.

Aursudkij, B., McDowell, G.R. and Collop, A.C. (2009). Cyclic loading of railway ballast under triaxial conditions and in a railway test facility. *Granular Matter,* **11**, 391–401.

Biabani, M.M., Ngo, N.T. and Indraratna, B. (2016). Performance evaluation of railway subballast stabilised with geocell based on pull-out testing. *Geotextiles and Geomembranes,* **44**(4), 579-591.

Bian, X., H. Jiang, C. Cheng, Y. Chen, R. Chen and J. Jiang (2014). Full-scale model testing on a ballastless high-speed railway under simulated train moving loads. Soil Dynamics and Earthquake Engineering 66: 368-384.

Bian, X., Gao, Y., Huang, H., and Xie, Y. (2017). Hanging tie study using the "moving deflection spectrum". Proceedings of the Institution of Mechanical Engineers, Part F: Journal of Rail and

Rapid Transit, 231(8): 982-990.

Bian, X., Li, W., Qian, Y. and Tutumluer, E. (2020). Analysing the effect of principal stress rotation on railway track settlement by discrete element method. *Géotechnique,* **0**(0), 1-19.

Brown, S.F., Brodrick, B.V., Thom, N.H. and McDowell, G.R. (2007). The Nottingham railway test facility, UK. *Proceedings of the Institution of Civil Engineers - Transport,* **160**(2), 59-65.

Brown, S.F., Kwan, J. and Thom, N.H. (2007). Identifying the key parameters that influence geogrid reinforcement of railway ballast. *Geotextiles and Geomembranes,* **25**(6), 326-335.

Budiono, D.S., McSweeney, T., Dhanasekar, M. and Gurung, N. (2004). "The effect of coal dust fouling on the cyclic behaviour of railtrack ballast." *Cyclic Behaviour of Soils and Liquefaction phenomena*, Taylor & Francis Group, London.

Cai, Y., L. Xu, W. Liu, Y. Shang, N. Su and D. Feng (2020). Field Test Study on the dynamic response of the cement-improved expansive soil subgrade of a heavy-haul railway. Soil Dynamics and Earthquake Engineering, 128: 105878.

Esveld, C. (2014). Modern railway track, MRT Press, The Netherlands.

Ferreira, F. and Indraratna, B. (2018). Deformation and degradation response of railway ballast under impact loading–effect of artificial inclusions. In ICRT 2017: Railway Development, Operations, and Maintenance - Proceedings of the 1st International Conference on Rail Transportation, p. 1090-1101.

Guo, Y., Fu, H., Qian, Y., Markine, V. and Jing, G. (2020). Effect of sleeper bottom texture on lateral resistance with discrete element modelling. *Construction and Building Materials,* **250**, 118770.

Harkness, J., Zervos, A., Le Pen, L., Aingaran, S. and Powrie, W. (2016). Discrete element simulation of railway ballast: modelling cell pressure effects in triaxial tests. *Granular Matter,* **18**(3), 65.

Hasnayn, M.M., McCarter, W.J., Woodward, P.K. and Connolly, D.P. (2020). Railway subgrade performance after repeated flooding–Large-scale laboratory testing. Transportation Geotechnics, 23, p.100329.

Huang, H., Tutumluer, E. and Dombrow, W. (2009). "Laboratory characterisation of fouled railroad ballast behavior." *Transportation Research Record: Journal of the Transportation Research Board, No. 2117*, Washington, DC.

Hu, P., Zhang, C., Wen, S., and Wang, Y. (2019). Dynamic responses of high-speed railway transition zone with various subgrade fillings. Computers and Geotechnics, 108: 17-26.

Indraratna, B., Salim, W., & Rujikiatkamjorn, C. (2011). Advanced Rail Geotechnology - Ballasted Track: CRC Press, Taylor & Francis Group, London, UK.

Indraratna, B., Ferreira, F.B., Qi, Y. and Ngo, T.N. (2018b). Application of geoinclusions for sustainable rail infrastructure under increased axle loads and higher speeds. *Innovative Infrastructure Solutions,* **3**(1), 69.

Indraratna, B., Lackenby, J. and Christie, D. (2005). Effect of confining pressure on the degradation of ballast under cyclic loading. *Géotechnique,* **55**(4), 325–328.

Indraratna, B., Ngo, N.T., Ferreira, F.B., Rujikiatkamjorn, C. and Shahkolahi, A. (2020a). Laboratory examination of ballast deformation and degradation under impact loads with synthetic inclusions. *Transportation Geotechnics,* **25**, 100406.

Indraratna, B., Ngo, N.T., Nimbalkar, S. and Rujikiatkamjorn, C. (2018a). Two Decades of Advancement in Process Simulation Testing of Ballast Strength, Deformation, and Degradation. ASTM-Railroad Ballast Testing and Properties. **1605:** 11-38.

Indraratna, B., Ngo, N.T. and Rujikiatkamjorn, C. (2013). Deformation of coal fouled ballast stabilized with geogrid under cyclic load. *Journal of Geotechnical and Geoenvironmental Engineering,* **139**(8), 1275-1289.

Indraratna, B. and Ngo, T. (2018). Ballast Railroad Design: Smart-Uow Approach, CRC Press.

Indraratna, B., Nimbalkar, S., Christie, D., Rujikiatkamjorn, C. and Vinod, J.S. (2010). Field assessment of the performance of a ballasted rail track with and without geosynthetics. *Journal of Geotechnical and Geoenvironmental Engineering,* **136**(7), 907–917.

Indraratna, B., Nimbalkar, S. and Neville, T. (2014). Performance assessment of reinforced ballasted rail track. *Proceedings of the Institution of Civil Engineers - Ground Improvement,* **167**(1), 24-34.

Indraratna, B., Nimbalkar, S.S., Ngo, N.T. and Neville, T. (2016). Performance improvement of rail track substructure using artificial inclusions: Experimental and numerical studies. *Transportation Geotechnics,* **8**, 69-85.

Indraratna, B., Qi, Y., Ngo, T.N., Rujikiatkamjorn, C., Neville, T., Ferreira, F.B. and Shahkolahi, A. (2019). Use of geogrids and recycled rubber in railroad infrastructure for enhanced performance. *Geosciences,* **9**(1).

Indraratna, B., Singh, M., Nguyen, T.T., Leroueil, S., Abeywickrama, A., Kelly, R. and Neville, T. (2020b). A laboratory study on fluidization of subgrade under cyclic train loading. *Canadian Geotechnical Journal*.

Kouroussis, G., Verlinden, O. and Conti, C. (2009). Ground propagation of vibrations from railway vehicles using a finite/infinite-element model of the soil. *Proceedings of the Institution of Mechanical Engineers, Part F: Journal of Rail and Rapid Transit,* **223**(4), 405-413.

Lade, P.V., Yamamuro, J.A. and Bopp, P.A. (1996). Significance of particle crushing in granular materials. *Journal of Geotechnical Engineering, ASCE,* **122**(4), 309-316.

Le Pen, L., Milne, D., Thompson, D. and Powrie, W. (2016). Evaluating railway track support stiffness from trackside measurements in the absence of wheel load data. *Canadian Geotechnical Journal,* **53**(7), 1156-1166.

Li, D., Hyslip, J., Sussmann, T. and Chrismer, S. (2015). Railway geotechnics, CRC Press.

Li, W., X. Bian, X. Duan and E. Tutumluer (2018). Full-Scale Model Testing on Ballasted High-Speed Railway: Dynamic Responses and Accumulated Settlements. Transportation Research Record 2672(10): 125-135.

Li, H., Z. Wang, F. Huang, Z. Yi, Y. Xie, D. Sun and R. Sun (2020). Impact of different lithological manufactured sands on high-speed railway box girder concrete. Construction and Building Materials, 230: 116943.

Lim, W.L., McDowell, G.R. and Collop, A.C. (2005). Quantifying the relative strengths of railway ballasts. *Geotechnical Engineering,* **158**(2), 107–111.

Marachi, N.D., Chan, C.K. and Seed, H.B. (1972). Evaluation of properties of rockfill materials. *Soil Mechanics and Foundations Division: Proceedings of the American Society of Civil Engineers,* **98**(SM1), 95-115.

Marsal, R.J. (1973). Mechanical properties of Rockfill. In : Embankment Dam Engineering Wiley, New York, pp: 109-200.

McDowell, G.R., Lim, W.L., Collop, A.C., Armitage, R. and Thom, N.H. (2005). Laboratory simulation of train loading and tamping on ballast. *Proceedings of the Institution of Civil Engineers: Transport,* **158**(TR2), 89-95.

Mishra, D., Qian,Y., Huang, H. and Tutumluer, E. (2014). An integrated approach to dynamic analysis of railroad track transitions behavior. Transportation Geotechnics 1(4): 188-200.

Navaratnarajah, S.K., Indraratna, B. and Ngo, N.T. (2018). Influence of Under Sleeper Pads on Ballast Behavior Under Cyclic Loading: Experimental and Numerical Studies. *Journal of Geotechnical and Geoenvironmental Engineering,* **144**(9), 04018068.

Nimbalkar, S. and Indraratna, B. (2016). Improved performance of ballasted rail track using geosynthetics and rubber shockmat. *Journal of Geotechnical and Geoenvironmental Engineering* **142**(8), 04016031.

Paixão, A., Fortunato, E. and Calçada (2016). A numerical study on the influence of backfill settlements in the train/track interaction at transition zones to railway bridges. Proceedings of the Institution of Mechanical Engineers, Part F: Journal of Rail and Rapid Transit ,230(3): 866-878.

Peijun, G. and Xubin, S. (2007). Shear strength, interparticle locking, and dilatancy of granular materials. *Canadian Geotechnical Journal,* **44**(5), 579.

Powrie, W., Le Pen, L., Milne, D. and Thompson, D. (2019). Train loading effects in railway geotechnical engineering: Ground response, analysis, measurement and interpretation. *Transportation Geotechnics,* **21**, 100261.

Powrie, W., Yang, L.A. and Clayton, C.R.I. (2007). Stress changes in the ground below ballasted railway track during train passage. *Proceedings of the Institution of Mechanical Engineers: Part F: Journal of Rail and Rapid Transit*, 247-261.

Priest, J.A., Powrie, W., Yang, L., Grabe, P.J. and Clayton, C.R.I. (2010). Measurements of transient ground movements below a ballasted railway line. *Geotechnique,* **60**(9), 667–677.

Raymond, G.P. and Bathurst, R.J. (1994). Repeated-load response of aggregates in relation to track quality index. *Canadian Geotechnical Journal,* **31**, 547-554.

Raymond, G.P. and Davies, J.R. (1978). Triaxial tests on dolomite railroad ballast. *Journal of the Geotechnical Engineering Division: Proceedings of the American Society of Civil Engineers,* **104**(GT6), 737-751.

Sayeed, M.A. and Shahin, M.A. (2016). Three-dimensional numerical modelling of ballasted railway track foundations for high-speed trains with special reference to critical speed. *Transportation Geotechnics,* **6**, 55-65.

Sayeed, M.A. and Shahin, M.A. (2017). Design of ballasted railway track foundations using numerical modelling. Part I: Development. *Canadian Geotechnical Journal,* **55**(3), 353-368.

Selig, E.T. and Waters, J.M. (1994). Track geotechnology and substructure management, Thomas Telford, London.

Sevi, A., Ge, L. and Take, W. (2009). A Large-Scale Triaxial Apparatus for Prototype Railroad Ballast Testing. *Geotechnical Testing Journal,* **32**(4), 297-304.

Sol-Sánchez, M., F. Moreno-Navarro, R. Tauste-Martínez, L. Saiz and M. C. Rubio-Gámez (2020). Recycling Tire-Derived Aggregate as elastic particles under railway sleepers: Impact on track lateral resistance and durability. Journal of Cleaner Production, 277: 123322.

Suiker, A.S.J. and Borst, R. (2003). A numerical model for the cyclic deterioration of railway tracks. *International Journal for Numerical methods in Engineering,* **57**, 441–470.

Suiker, A.S.J., Selig, E.T., and Frenkel, R. (2005). Static and cyclic triaxial testing of ballast and subballast. Journal of Geotechnical and Geoenvironmental Engineering, 131(6): 771–782.

Sun, Q., Indraratna, B. and Ngo, N.T. (2019). Effect of increase in load and frequency on the resilience of railway ballast. *Géotechnique,* **69**(9), 833-840.

Sun, Q. D., B. Indraratna and S. Nimbalkar (2016). Deformation and Degradation Mechanisms of Railway Ballast under High Frequency Cyclic Loading. Journal of Geotechnical and Geoenvironmental Engineering, 142(1): 04015056.

Touqan, M., A. Ahmed, H. El Naggar and T. Stark (2020). Static and cyclic characterization of fouled railroad sub-ballast layer behaviour. Soil Dynamics and Earthquake Engineering, 137: 106293.

Wang, T., Luo, Q., Liu, M., Wang, L. and Qi, W. (2020). Physical modeling of train-induced mud pumping in substructure beneath ballastless slab track. *Transportation Geotechnics,* **23**, 100332.

Zhai, W.M., Wang, K.Y. and Lin, l.H. (2004). Modelling and experiment of railwayballast vibrations. *Journal of Sound and Vibration,* **673–683**, 673–683.

Zhai, W., Wang, K., Chen, Z., Zhu, S., Cai, C. and Liu, G. (2020). Full-scale multi-functional test platform for investigating mechanical performance of track-subgrade systems of high-speed railways. Railway Engineering Science, 28(3): 213-231.

Zhang, X., C. Zhao and W. Zhai (2017). Dynamic behavior analysis of high-speed railway ballast under moving vehicle loads using discrete element method." International Journal of Geomechanics 17(7): 04016157.

Zhang, X., Zhao, C., Zhai, W. and Shi, C. (2019a). Investigation of track settlement and ballast degradation in the high-speed railway using a full-scale laboratory test. Proceedings of the Institution of Mechanical Engineers, Part F: Journal of Rail and Rapid Transit, 233(8): 869-881.

Zhang, X., C. Zhao and W. Zhai (2019b). Importance of load frequency in applying cyclic loads to investigate ballast deformation under high-speed train loads. Soil Dynamics and Earthquake Engineering 120: 28-38.

Table 1. Quantification of ballast breakage (*BBI*) recovered at different places after the test

Sieve size (mm)	**Passing (%)**				
	Initial gradation of tested ballast	Collected ballast underneath the South-East actuator	Collected ballast underneath the North-West actuator	Collected ballast between two rails	Collected ballast at the end of sleeper (shoulder ballast)
63	100	100	100	100	100
53	93.75	94.2	94.50	94.2	93.9
37.5	51.70	63.5	61.20	56.2	55.7
26.5	21.38	31.4	31.20	27.9	27.2
19	5.92	10.9	10.53	10.36	9.8
13.2	2.68	8.5	7.47	6.98	6.52
9.5	2.15	6.12	5.67	4.78	4.25
4.75	1.83	3.12	3.73	3.14	2.04
2.36	0	0	0	0	0
	Measured *BBI*	**0.143**	**0.115**	**0.085**	**0.074**

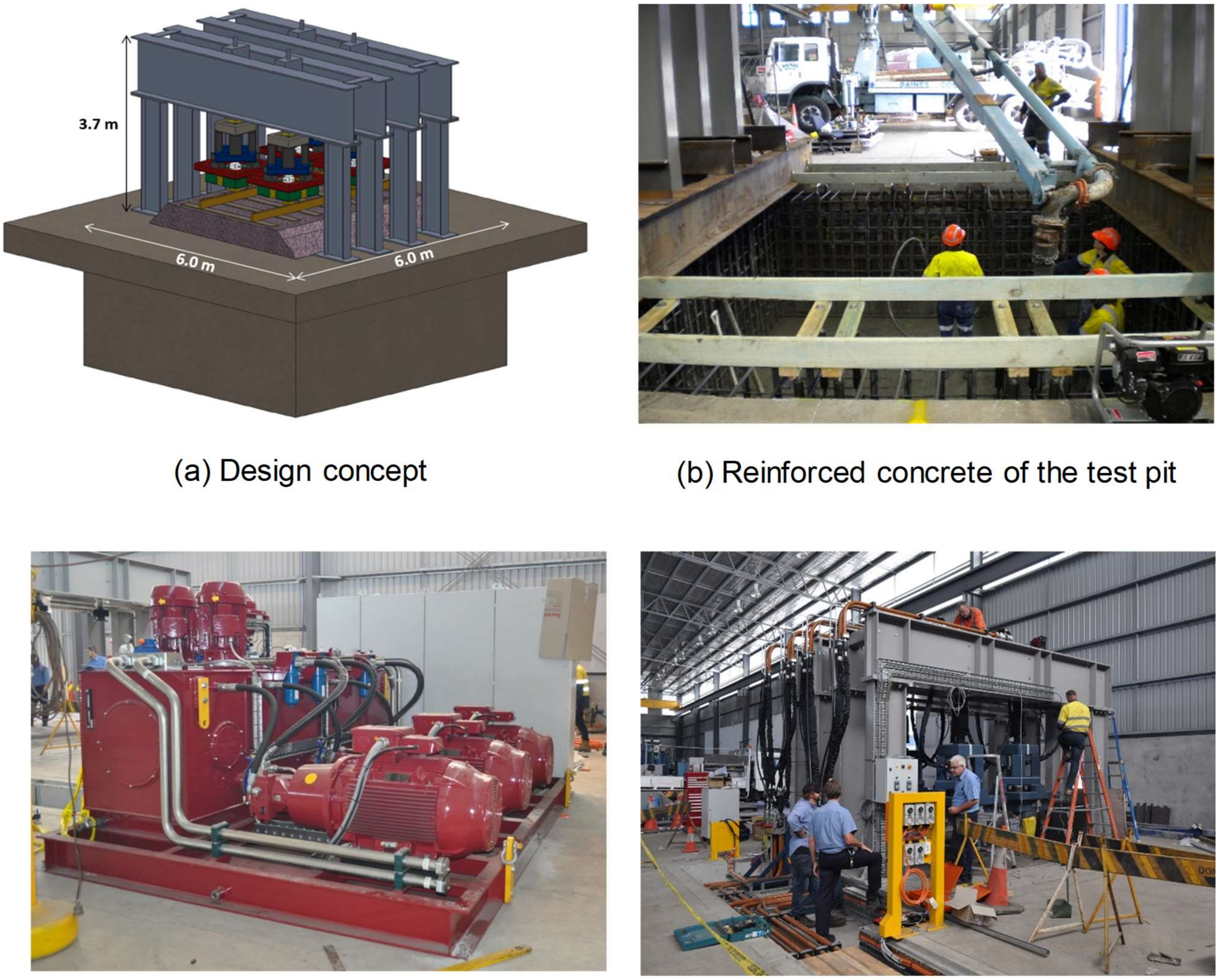

(a) Design concept

(b) Reinforced concrete of the test pit

(c) Hydraulic power unit

(d) Hydraulic pipe system

Figure 1. Design and construction of the NFHRT

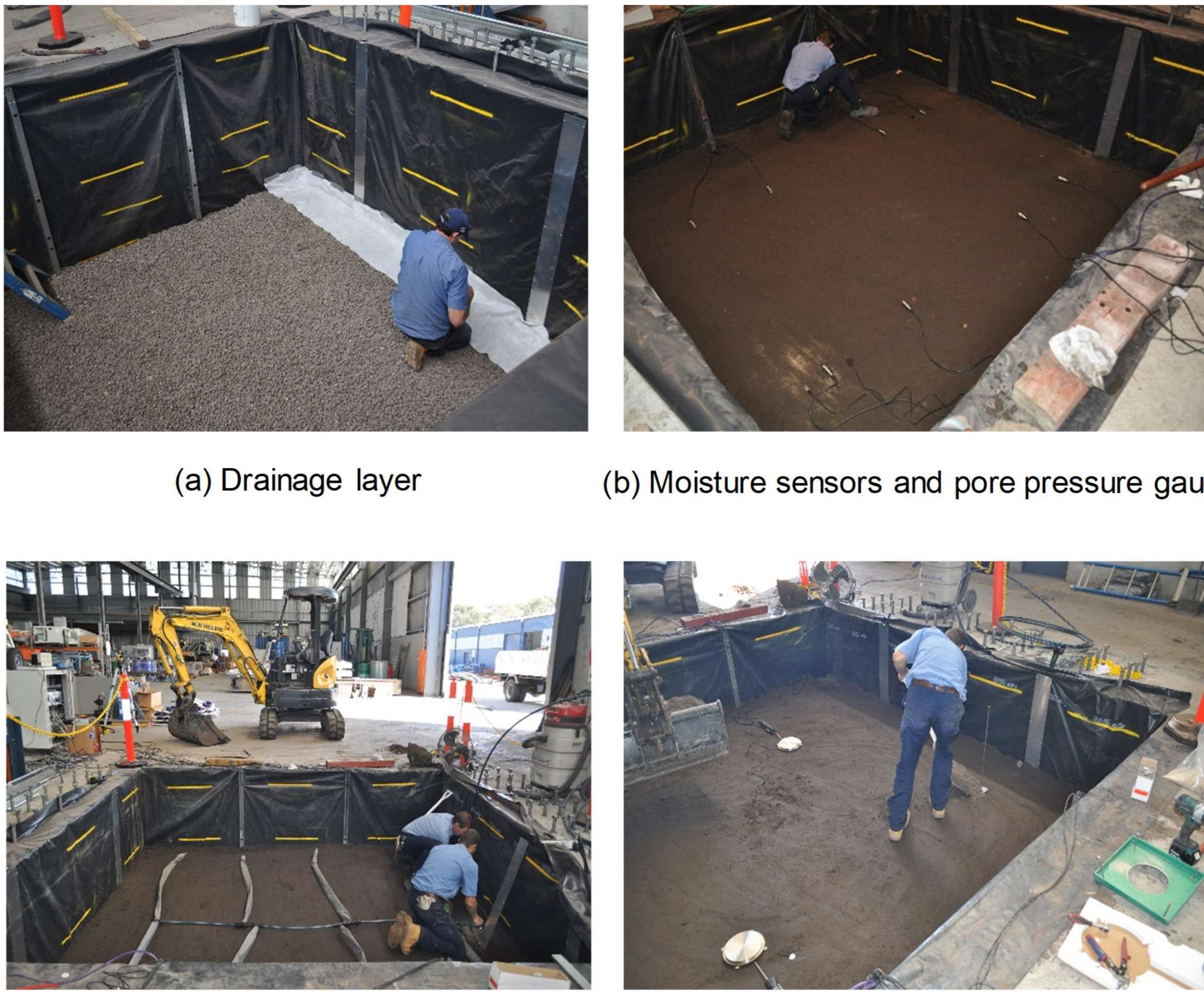

(a) Drainage layer
(b) Moisture sensors and pore pressure gauges
(c) Irrigation system
(d) Pressure cells on top of subgrade

Figure 2. Installation of the drainage and subgrade layers

(a) Capping layer

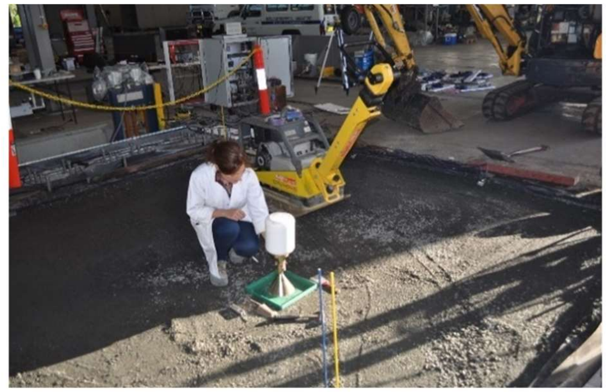

(b) Sand-cone test for compacted capping

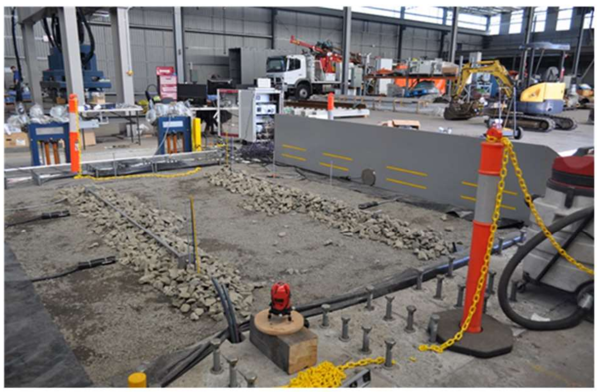

(c) Placement of ballast

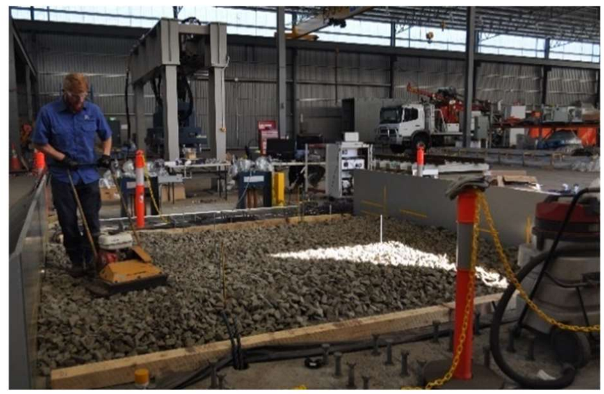

(d) Compaction of ballast layer

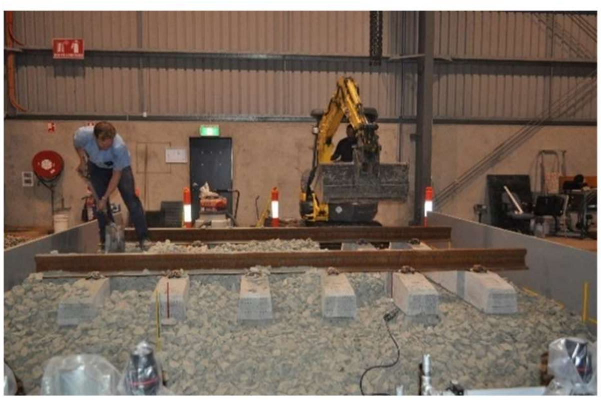

(e) Rails and sleepers

(f) Loading frames and hydraulic actuators

Figure 3. Installation of the capping, ballast, rail-sleeper assembly and dynamic actuators

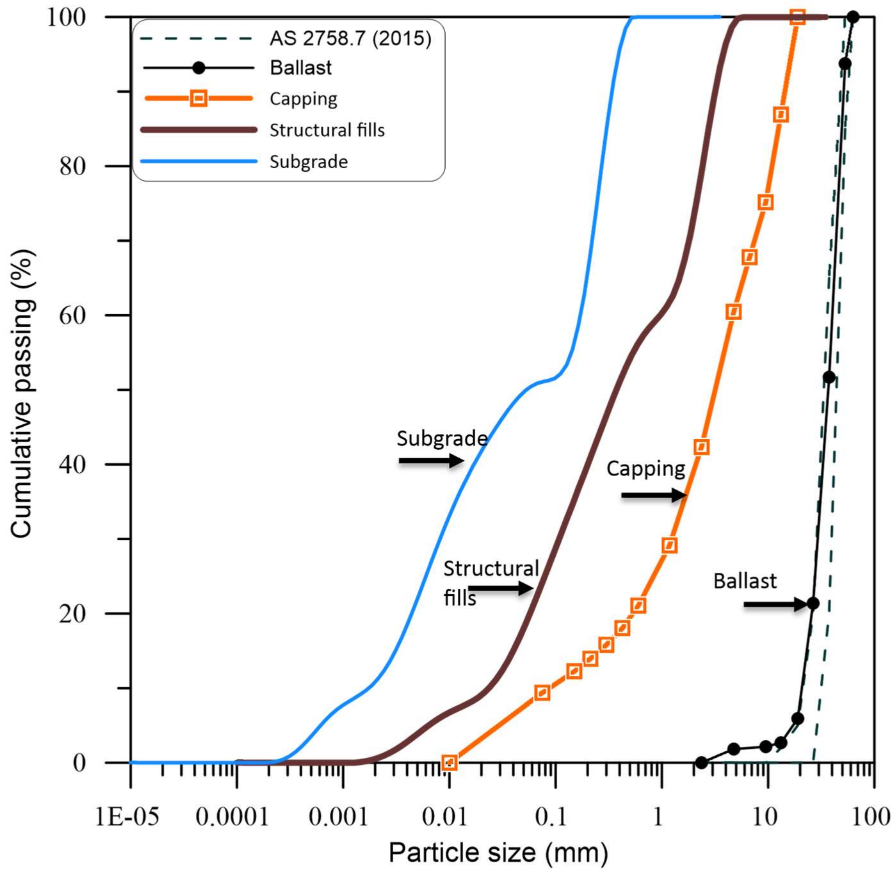

Figure 4. Particle size distribution curves of the track substructure materials

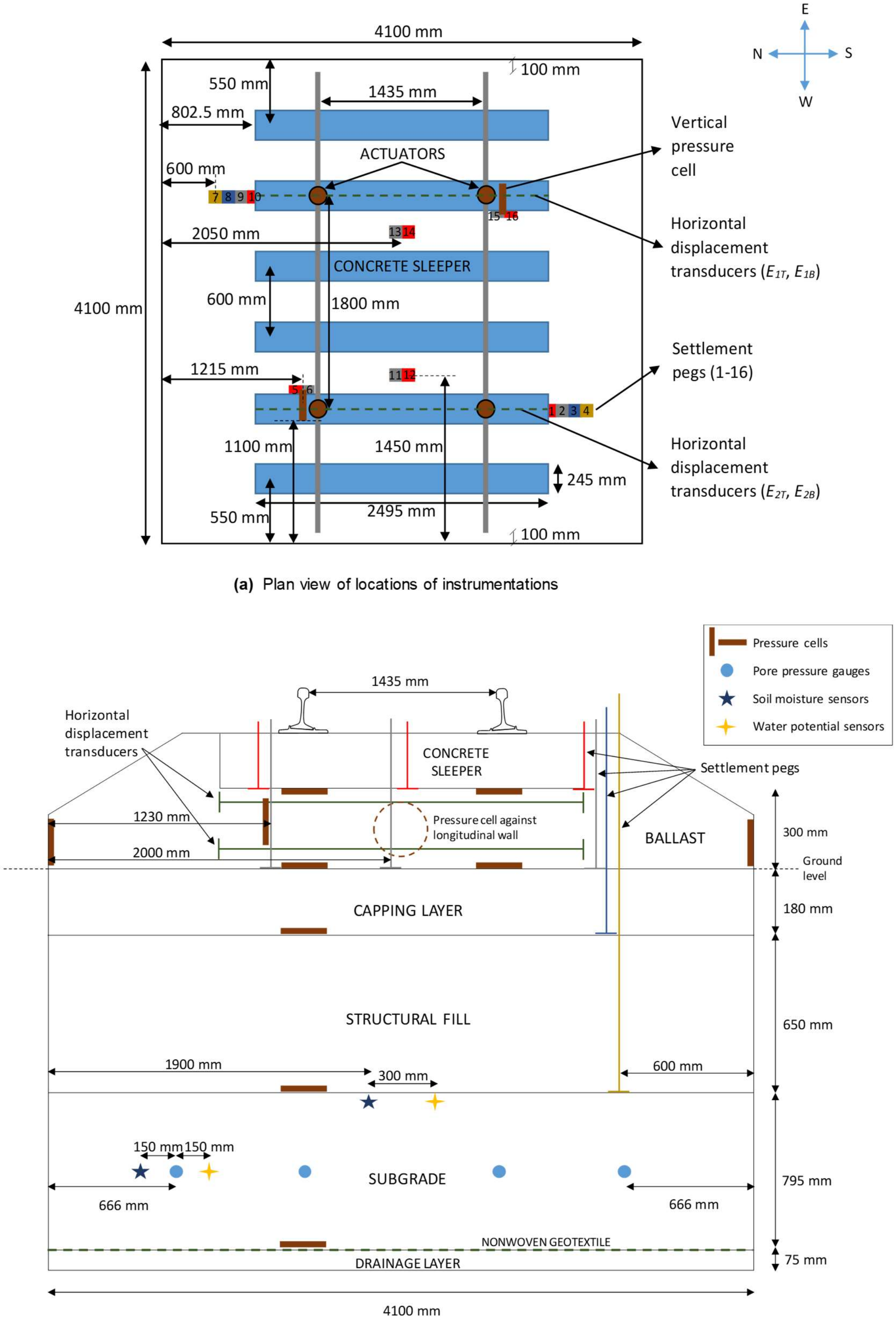

(a) Plan view of locations of instrumentations

(b) A cross-section of the test pit with detailed instrumentations

Figure 5. A plan view and cross-section of the NFHRT with detailed instrumentations

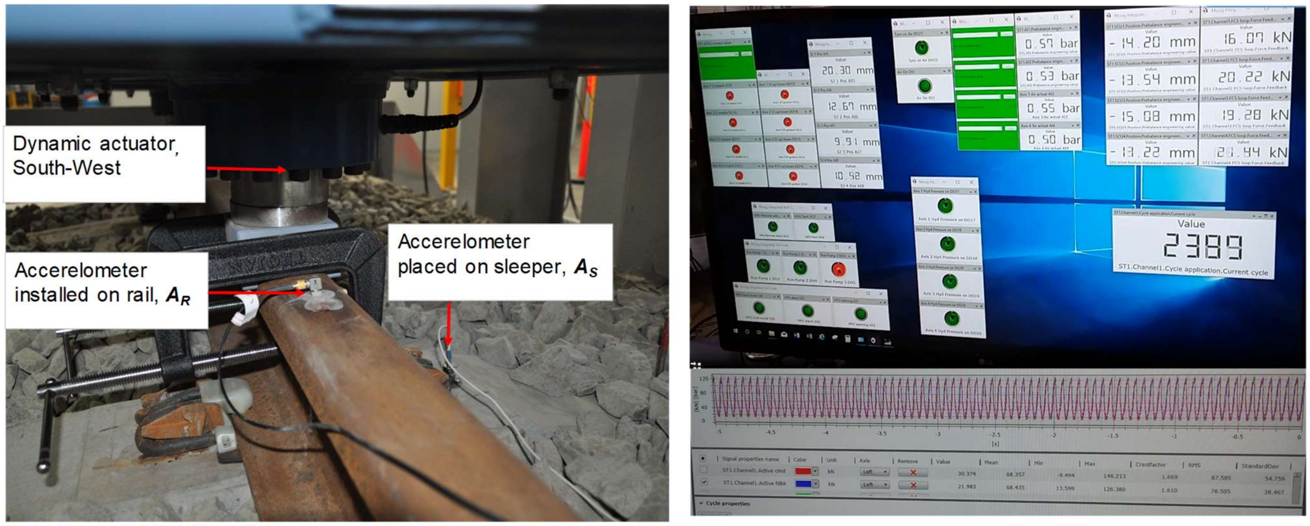

(a) (b)

Figure 6. (a) Installation of triaxial accelerometers on the rail and sleeper; (b) data acquisition system

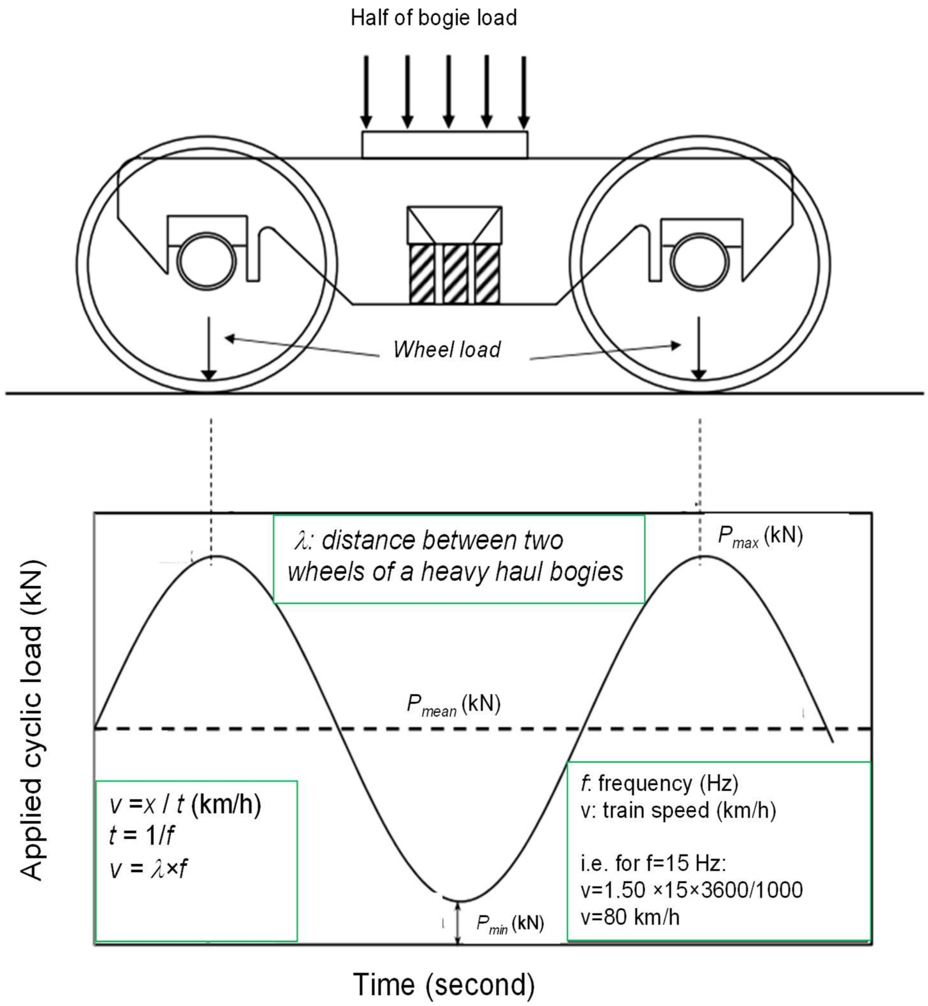

Figure 7. Typical schematic of axle load and applied cyclic load during the test

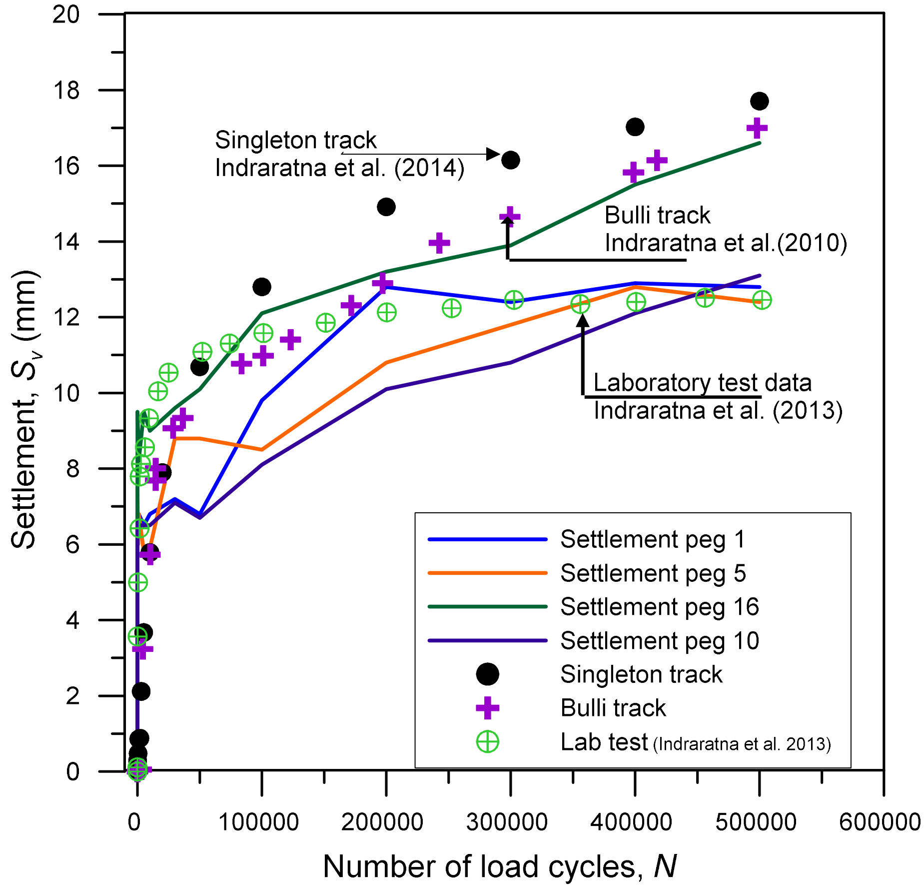

Figure 8. Measured settlements of the track at different locations in comparison with laboratory and field measurement data

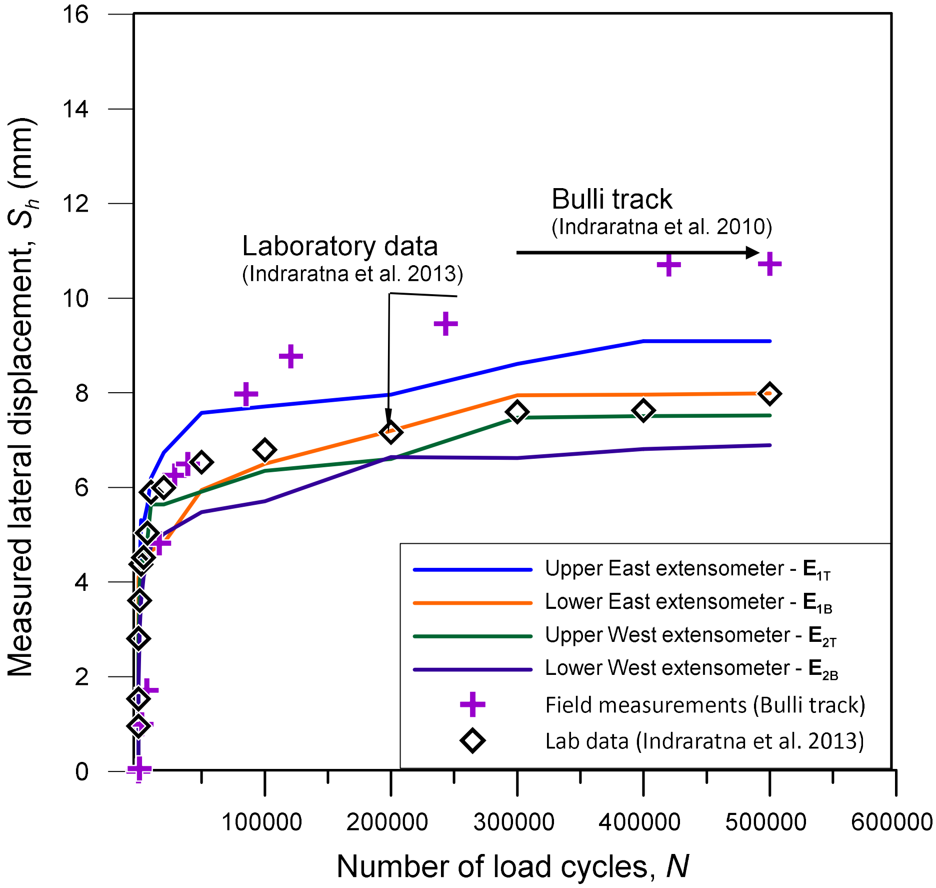

Figure 9. Measured lateral displacements at varying locations in comparison with laboratory and field measurement data

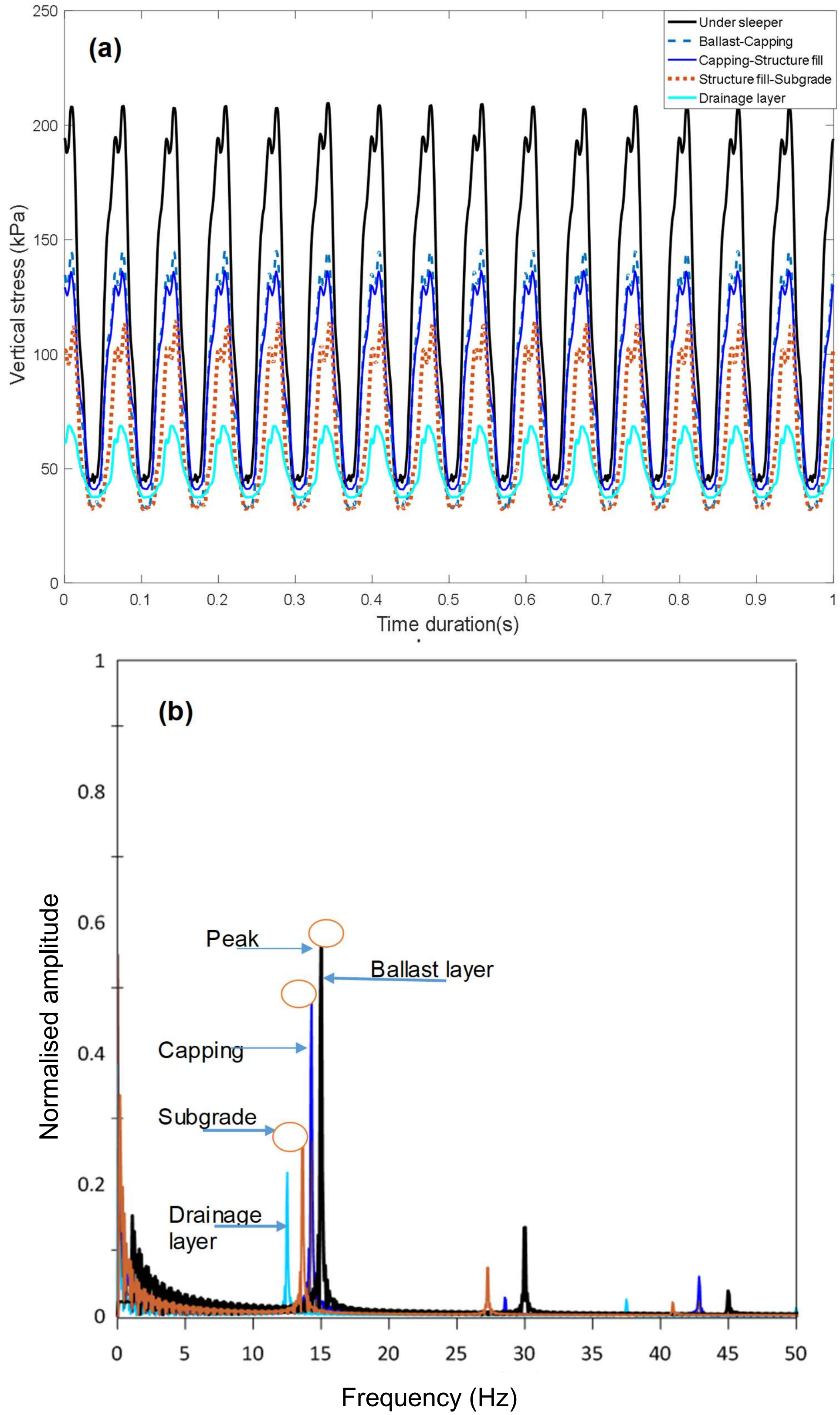

Figure 10. Typical cyclic vertical stress (σ_1) responses at varying depths measured by pressure plates: (a) time domain; (b) frequency domain

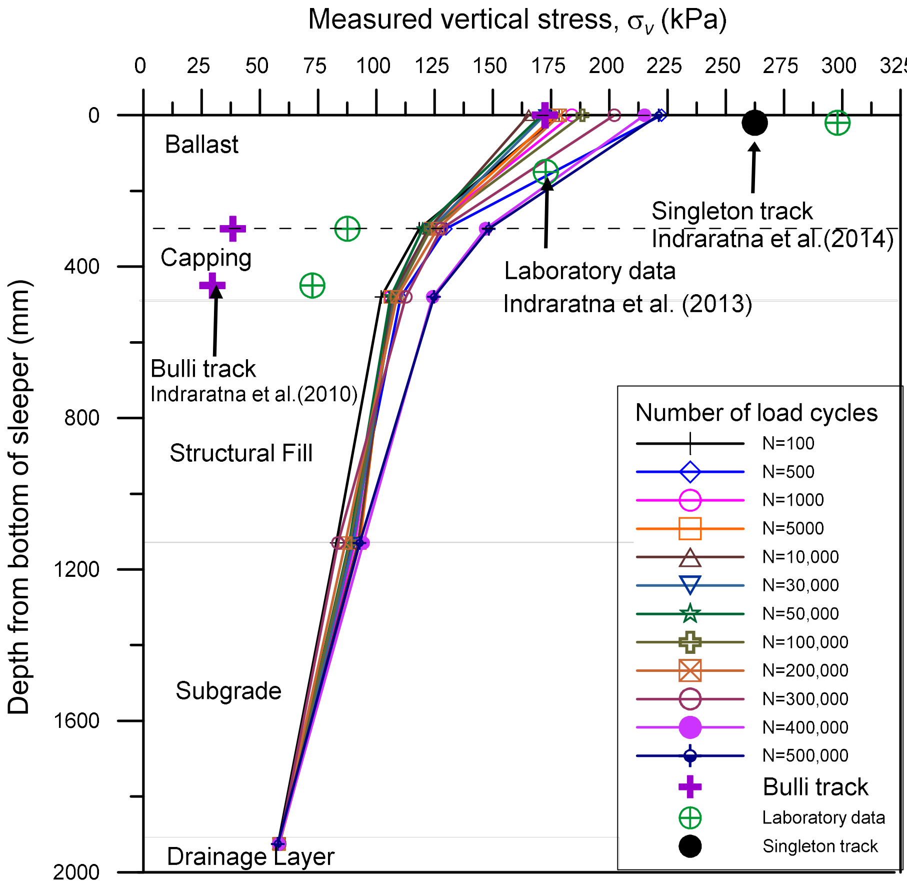

Figure 11. Variations of measured vertical stress (σ_v) with the depth of track substructure at varying load cycles (N)

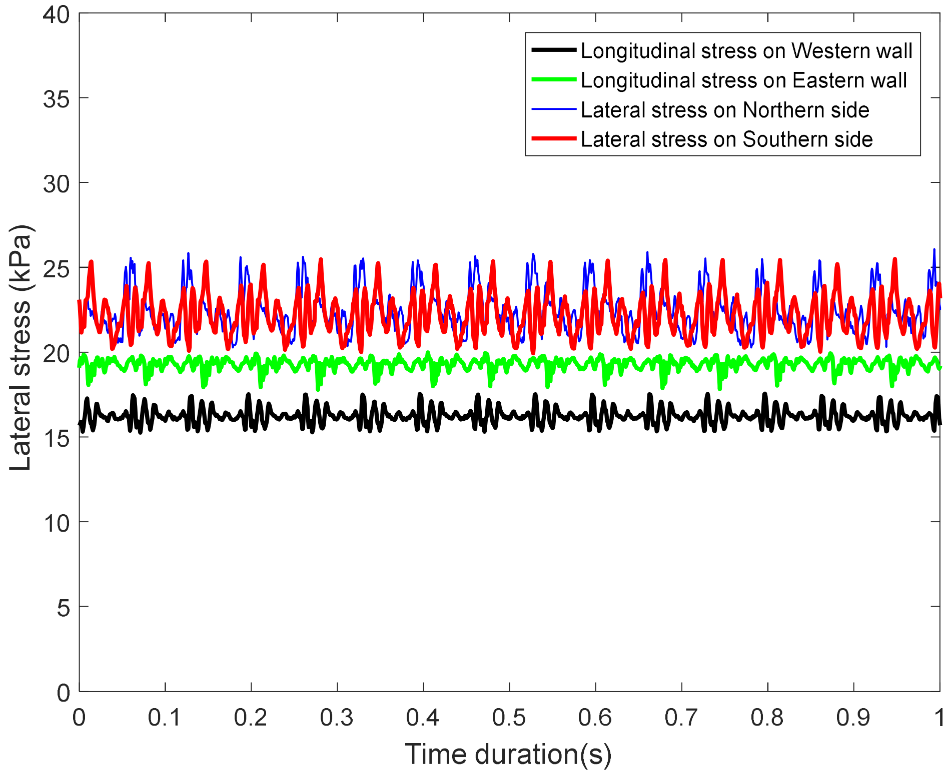

Figure 12. Typical responses of horizontal stresses (σ_2, σ_3) in ballast measured in longitudinal and transverse directions during the test

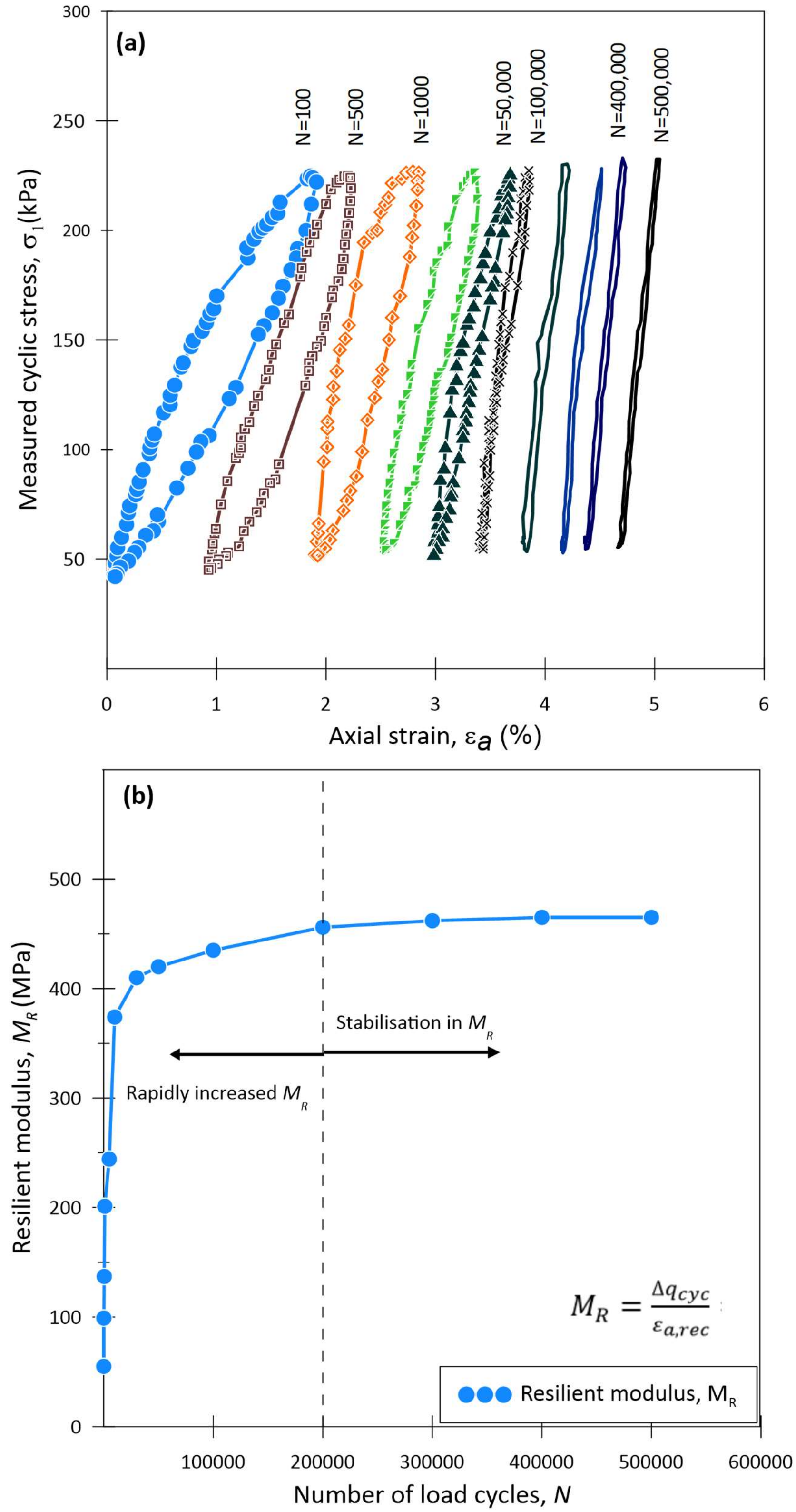

Figure 13. (a) Hysteresis cyclic stress– strain responses; and (b) measured resilient modulus (M_R)

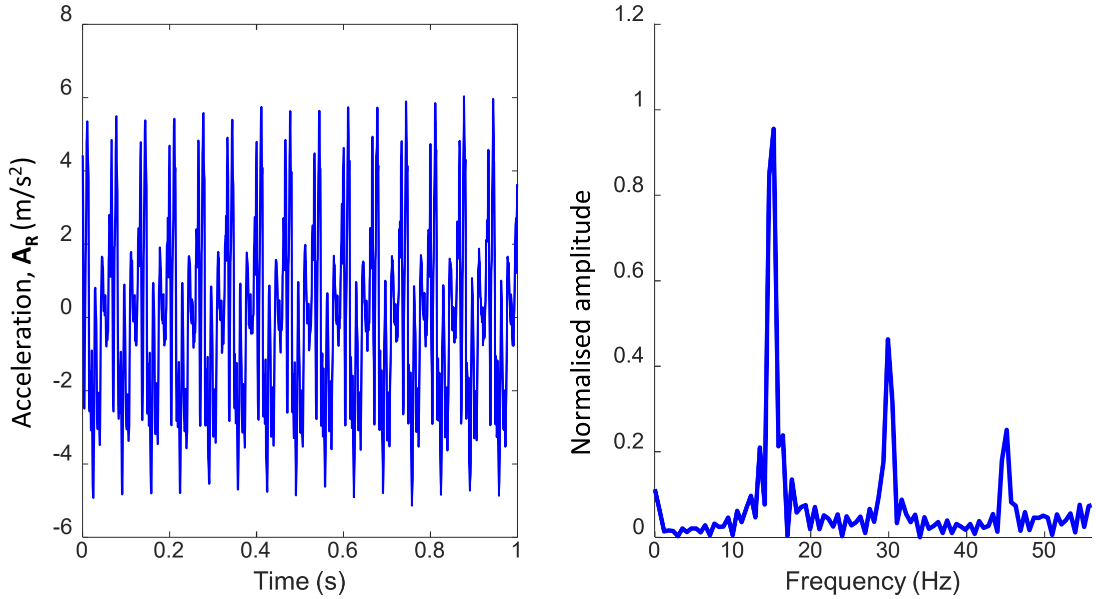

(a) Measured accelerations on rail

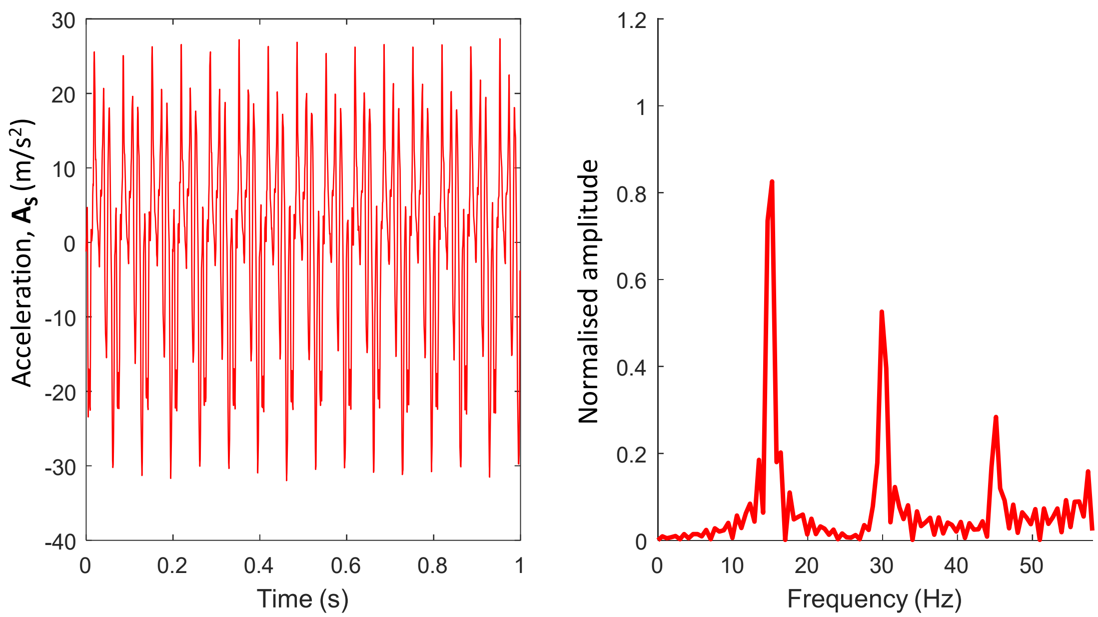

(b) Measured accelerations on sleeper

Figure 14. Measured accelerations of rail and sleeper during the test

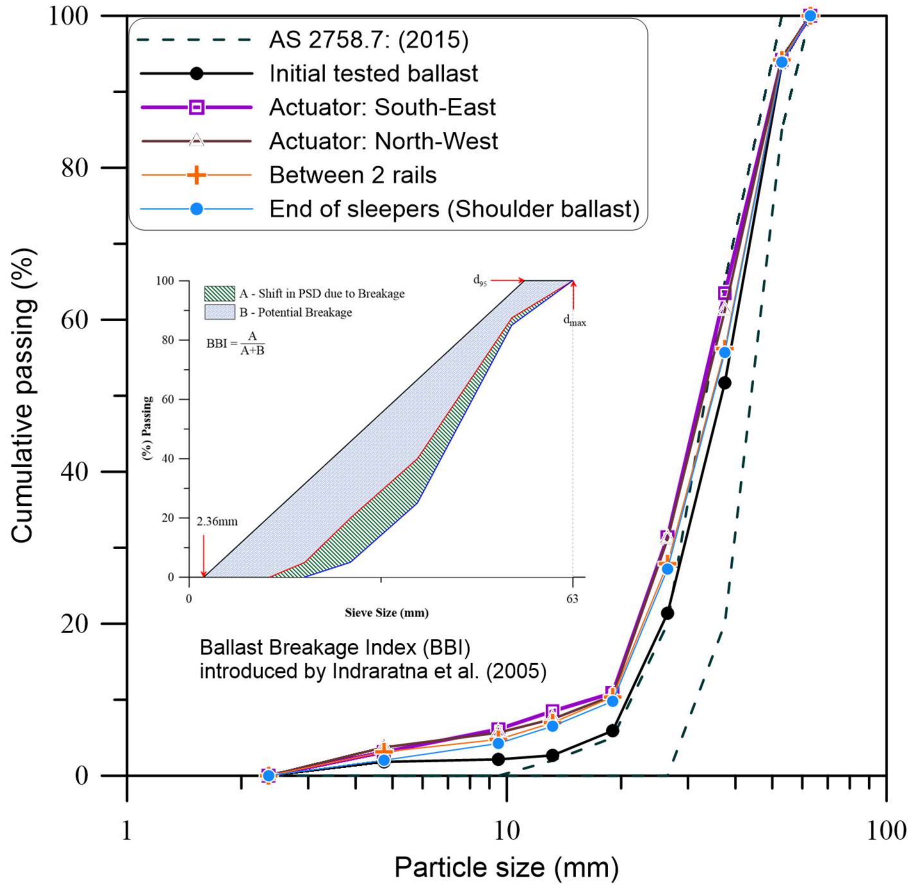

Figure 15. Measured changes in particle size distributions of ballast for quantifying ballast breakage index (*BBI*)

Transportation Geotechnics

Authors Responses to Review Comments to Manuscript ID: TRGEO-D-20-00552R1

Paper title: Large-scale Testing Facility for Heavy Haul Track

Authors: Buddhima Indraratna, Trung Ngo, Fernanda Ferreira, Cholachat Rujikiatkamjorn, and Ameyu Tucho

Reviewer #3: *The manuscript has been well revised according to reviewer's recommendations.*

I still don't agree the statemen that cyclic loads with the frequency of 15 Hz are equivalent to train loads with a speed of 80km/h, because it is not be verified by the authors. There are several constant spacing distances for a certain train, the highest passing frequency (corresponding to the 1.5m wheel base) cannot represent the actual frequency characterstics, and a load sequence with the rest times should be more appropriate. Additionally, for the heavy haul railway(<120km/h), many previous reseaches showed that the axle load and the number of axes passing through the worksite is important to track settlement, not the runing speed of train. A numerial simuations showed that if the frequency of periodic harmonic loads is considerable high, the settlement trend of track model is quite different. In terms of the laboratory model experiment, using high frequency cyclic loads still cannot obtain accurately track dynamic response, because dynamic effect due to the track irregularities can not be considered reasonably in the actuators. Thus, I think the load frequency should not be discussed too much in this manuscript.

Response: The authors appreciate the Review comments that help to significantly improve the quality and flow of the re-revised final manuscript.

Regarding the loading frequency, the authors wish to clarify that heavy haul trains in Australia are often 4-5 km long and they travel on standard gauge tracks at relatively low speed (@ 40-60 km/h in most cases and rarely exceed 70k/h), and the applied frequency in the laboratory is indeed corroborated with the track geometry and train speed (e.g. Indraratna et al. 2011, Sun et al. 2016, Navaratnarajah et al. 2018). The authors agree that there can be several variables including the sleeper spacing, speed of train, track irregularities, occasional impact loading, influence of rest periods, variation in cyclic loading due to non-uniform axle spacing etc. that can contribute to the real-life frequency in contrast to the simplified (constant) experimental magnitude of frequency. To avoid confusion, the statement "*a frequency of 15 Hz to simulate to simulate a freight train travelling at approximately v = 80 km/h*" has now been amended. Instead, it is mentioned that: "The applied frequency of 15 Hz in the experimental program is assumed to cover a realistic range of heavy haul train speeds of 60-80km/h on standard gauge tracks, based on Indraratna et al. (2011), Sun et al. (2016) and Navaratnarajah et al. (2018) I reality, the frequency is not only dependent on the train speed but also on track geometry, bogey spacing, rest periods, variations in cyclic and impact loading among other variables. (**Page 9, Para 1**).

In addition, it is noted that the loading sequence capturing rest periods is not considered in this study. This is because the worst conditions occur when very long heavy haul trains apply continual loading over a substantial period of time, and busy freight tracks in the mining hubs have relatively small rest periods. For example in Western Australia different mineral ore trains can travel over very long distances at slow speeds (40-60 km/h) from source to port (sometimes up to 300 km) regularly most of the day, and the ballast relaxation during relatively short rest periods between these slow-moving trains can be ignored. For instance for iron ore trains that can be up to 6 km long moving at only 40 km/h, the worst-case scenario simulated in the laboratory is without any rest period, so that the fatigue of ballast is maximised during testing to determine the maximum deformation, i.e. settlement and lateral movement.

The above statement has now included in the Loading Section of the revised manuscript (**Page 9, Para 2**).

The dynamic and impact effects due to track irregularities could not be captured in these model tests, and the authors have included this as a limitation of the current study (**Page 5, Para 2**)

The Authors agree with the Reviwer that both the axle load and loading frequency influence the resulting settlement, but the axle load magnitude is more dominant than the frequency. Nevertheless, the load frequency must still be highlighted, because that is the only loading parameter in cyclic laboratory testing that is related to the train speed (Esveld, 2014; Indraratna et al. 2011). In other words, the number of axle loads passing through a specific in situ reference point (worksite) over a given period of time is related to the frequency. This is clarified on **Page 9, Paragraph 2.**

References:

Esveld, C. (2014). Modern railway track: MRT Press, The Netherlands.

Indraratna, B., W. Salim and C. Rujikiatkamjorn (2011). Advanced Rail Geotechnology - Ballasted Track, CRC Press, Taylor & Francis Group, London, UK.

Navaratnarajah, S. K., B. Indraratna and N. T. Ngo (2018). Influence of Under Sleeper Pads on Ballast Behavior Under Cyclic Loading: Experimental and Numerical Studies. *Journal of Geotechnical and Geoenvironmental Engineering*, 144(9): 04018068.

Sun, Q. D., B. Indraratna and S. Nimbalkar (2016). Deformation and Degradation Mechanisms of Railway Ballast under High Frequency Cyclic Loading. *Journal of Geotechnical and Geoenvironmental Engineering*, 142(1): 04015056.